Changes to the Operational ''Early'' Eta Analysis/Forecast System at the National Centers for Environmental Prediction

ERIC ROGERS, THOMAS L. BLACK, DENNIS G. DEAVEN, AND GEOFFREY J. DIMEGO

Environmental Modeling Center, National Centers for Environmental Prediction, NWS/NOAA, Washington, D.C.

QINGYUN ZHAO AND MICHAEL BALDWIN

General Sciences Corporation, Laurel, Maryland

NORMAN W. JUNKER

Hydrometeorological Prediction Center, National Centers for Environmental Prediction, Washington, D.C.

YING LIN

University Corporation for Atmospheric Research, Boulder, Colorado

6 October 1995 and 29 January 1996

ABSTRACT

This note describes changes that have been made to the National Centers for Environmental Prediction (NCEP) operational ''early'' eta model. The changes are 1) an decrease in horizontal grid spacing from 80 to 48 km, 2) incorporation of a cloud prediction scheme, 3) replacement of the original static analysis system with a 12-h intermittent data assimilation system using the eta model, and 4) the use of satellite-sensed total column water data in the eta optimum interpolation analysis. When tested separately, each of the four changes improved model performance. A quantitative and subjective evaluation of the full upgrade package during March and April 1995 indicated that the 48-km eta model was more skillful than the operational 80-km model in predicting the intensity and movement of large-scale weather systems. In addition, the 48-km eta model was more skillful in predicting severe mesoscale precipitation events than either the 80-km eta model, the nested grid model, or the NCEP global spectral model during the March–April 1995 period. The implementation of this new version of the operational early eta system was performed in October 1995.

1. Introduction

The National Centers for Environmental Prediction (NCEP, formerly the National Meteorological Center) began production of operational forecasts from an 80-km, 38-level version of the eta model in June 1993, replacing the Limited-Area Fine-Mesh Model in providing ''early'' forecast guidance over North America. The June 1993 version of the so-called early eta system, as described by Black et al. (1993), consists of two components: a regional optimum interpolation (ROI) (DiMego 1988) analysis using a 6-h forecast of the NCEP global spectral model from the Global Data Assimilation System (GDAS; Kanamitsu et al. 1991) as a first guess, followed by a 48-h forecast of the eta coordinate model (Mesinger 1984). The early eta system was changed in September 1994 (Rogers et al. 1995) to include a more realistic depiction of the model orography and to improve the ROI analysis in the lower troposphere.

The purpose of this note is to describe changes to the early eta system that were implemented in October 1995. This upgrade consists of four components:

1) a decrease in horizontal grid spacing from 80 to 48 km,
2) incorporation of a cloud prediction scheme in the eta model physical package,
3) use of an eta-based intermittent data assimilation system to provide initial conditions to the eta model, and
4) use of satellite-sensed total column water data in the eta ROI analysis.

A description of each component of the early eta upgrade package and its impact on model performance

Corresponding author address: Dr. Eric Rogers, Environmental Modeling Center, National Centers for Environmental Prediction, WINP22, WWB, Room 204, Washington, DC 20233.
E-mail: wd20er@sun1.wwb.noaa.gov

TABLE 1. 48-km eta model characteristics.

Dynamics
Horizontal Arakawa E-grid, rotated spherical coordinates
Lorenz vertical grid; model top = 25 mb; step-mountain (eta) vertical coordinate (Mesinger 1984; Mesinger et al. 1988), 38 layers
Atmospheric prognostic variables: *u*, *V*, *T*, *q*, *q*2 (turbulence velocity squared), *m* (cloud water–ice mixing ratio), surface pressure
Split explicit time differencing (Janjić et al. 1995) with an adjustment time step of 120 s
Space differencing: conserving Arakawa-type scheme (Janjić 1984)
Arakawa (Arakawa and Lamb 1977) vertical advection except for moisture; piecewise-linear (e.g., van Leer 1977) vertical moisture advection
Gravity wave coupling scheme (Mesinger 1973; Janjić 1979)
Silhouette-mean orography (Mesinger 1995)
Energy conservation in transformations between kinetic and potential energy, in both space and time differencing (Mesinger et al. 1988; Janjić et al. 1995)
Physics
Modified Betts–Miller scheme for deep and shallow convection (Betts 1986; Betts and Miller 1986; Janjić 1994)
Explicit prediction of grid-scale cloud water/ice mixing ratio (Zhao et al. 1995), with predicted clouds used by the radiation scheme
Mellor–Yamada (1982) level-2.5 model for free atmosphere vertical turbulent exchange above lowest model layer
Geophysical Fluid Dynamics Laboratory radiation scheme (Fels and Schwarztkopf 1975; Lacis and Hansen 1974)
Viscous sublayer over water surfaces (Janjić 1994)
Surface layer: similarity functions derived from Mellor–Yamada level-2.0 model (Łobocki 1993)

is presented in section 2. The results of an objective verification of the upgrade package versus the 80-km version of the early eta, a subjective evaluation of the 48-km eta model, and two forecast examples are given in section 3. A summary follows in section 4.

2. Changes to the early eta system

This section describes changes to both the model and analysis components of the early eta system. A general description of the eta coordinate and the structure of the vertical and horizontal grids can be found in Black (1994). Table 1 lists the dynamical and physical package in the 48-km version of the eta model as implemented in October 1995. For more details concerning eta model dynamics and physics refer to the references listed therein.

a. Horizontal resolution

The main purpose for decreasing the horizontal grid spacing of the operational eta model is to provide forecasters with improved early guidance over all of North America. Since the operational 29-km mesoscale eta system (Black 1994), which NCEP has run twice daily since 28 March 1995, does not include Alaska, the upgrade of the early eta system to 48-km grid spacing satisfies NCEP's commitment to produce high-resolution forecasts for that state. As shown in Fig. 1a, the 48-km domain is nearly identical to the current 80-km domain (see Fig. 2a of Black et al. 1993). Although a smaller grid spacing such as 40 km would be preferable, a 40-km grid covering the domain depicted in Fig. 1a has 23% more grid points, which would tax NCEP's computer resources. For this reason, 48-km grid spacing was chosen.

The vertical resolution of the upgraded early eta system remains at 38 levels, with the pressure at the top of the model raised from 50 to 25 mb. The vertical distribution of these layers is shown in Fig. 1b. The highest resolution is seen in the boundary layer, where the lowest layer is defined to be exactly 20 m deep for the standard atmosphere. A secondary maximum appears near the tropopause for the purpose of better resolving jet stream features.

An obvious consequence of the increase in horizontal grid spacing is greater detail in the model orography, shown for both 80- and 48-km grid spacing in Fig. 2 over the western United States, eastern United States, and Alaska. While both grids are able to resolve the two highest peaks in the Alaskan region (Fig. 2c), Mt. McKinley (elevation 6194 m) and Mt. Logan in extreme southwestern Yukon (elevation 5867 m), the model elevation at both locations is 800–1000 m higher at 48-km grid spacing.

According to Mesinger and Baldwin (1995), increasing the horizontal resolution of the eta model tends to improve model accuracy in forecasting precipitation, based on the evaluation of quantitative precipitation scores. A recent comparison of the equitable threat score (ETS, defined in the appendix) (Schaefer 1990; Gandin and Murphy 1992; Mesinger and Black 1992) and bias score for 24-h precipitation amount from both the 80-km early eta and an experimental 40-km version is presented in Fig. 3. The 40-km eta forecast model differed from the 80-km early eta only in the horizontal resolution of the model, although the 40-

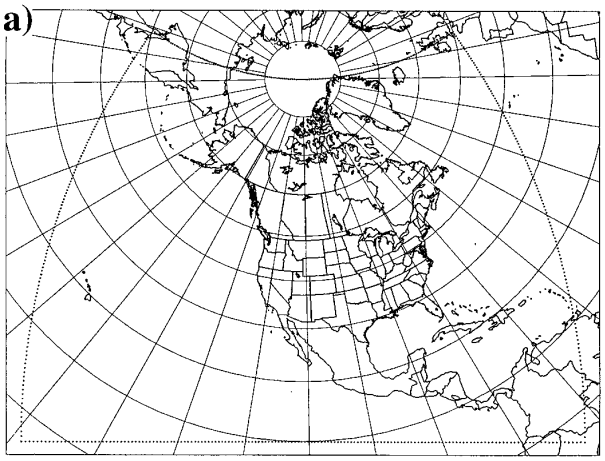

FIG. 1. (a) The horizontal domain of the 48-km eta model.

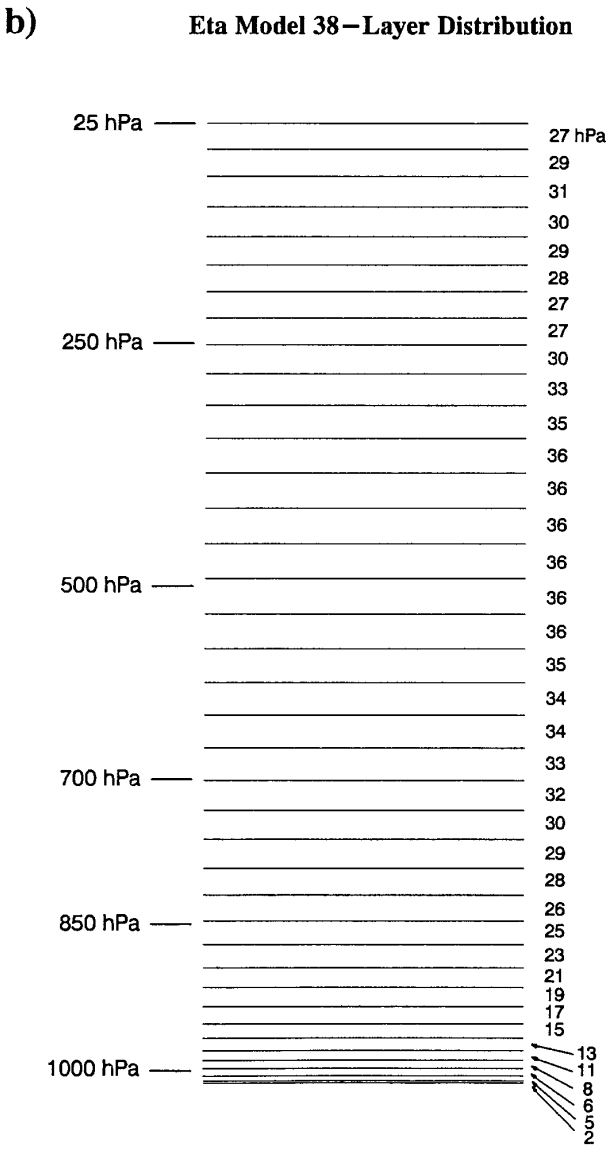

FIG. 1. (b) The distribution of the 38 layers in the 48-km eta model. The pressures on the left side indicate the layers' positions with respect to the standard atmosphere, while the numbers on the right give an approximate pressure depth of each layer in hectopascals.

km grid domain, while covering most of North America, is smaller than the 80-km domain. Verification is provided by an analysis of the Office of Hydrology's River Forecast Center 24-h observed precipitation data over the contiguous United States. The analysis is performed on the 80-km eta model grid, and the 40-km forecasts are remapped to the 80-km grid for verification by an area-integral method that conserves total water. All precipitation observations inside a grid box are averaged to produce the analyzed precipitation amount at each grid point. Figure 3 shows that the higher-resolution forecasts have slightly higher ETS at all precipitation amount thresholds, with greater impact at the lighter amounts. Both Black (1994) and Mesinger and Baldwin (1995) reported a similar impact from experimental 40-km eta model forecasts during 1992 and 1993 (not shown). The improved threat scores from the 40-km forecast are a sharp contrast to that model's bias score, which show a significant decrease in bias compared to the 80-km early eta at thresholds > 0.5 in. Figure 3 clearly shows that the increase in resolution caused a significant underprediction of precipitation during the 6-week test period in the fall of 1994. Evidence of the underprediction of 24-h precipitation amounts > 0.5 in. by the 40-km eta model was shown by Black (1994) in precipitation statistics from November 1993.

b. Prognostic cloud scheme

The June 1993 version of the 80-km eta model used the diagnostic scheme described by Hoke et al. (1989) for the production of large-scale condensation and precipitation. In this method, condensation is allowed to occur at a model grid point when the relative humidity exceeds a predefined critical value (95%). The condensation is summed layer by layer downward from the top, with water evaporated into subsaturated layers and temperature/specific humidity changed accordingly. Large-scale precipitation is defined as the water that reaches the ground as the result of this scheme.

Although the 80-km early eta system produced improved precipitation forecasts over other NCEP models using this simple scheme (Black et al. 1993; Mesinger and Baldwin 1995), clouds were completely ignored. At higher model resolutions, the neglect of clouds may adversely impact the prediction of precipitation, as Fig. 3 suggests. As the important role clouds play in atmospheric processes became more apparent (especially

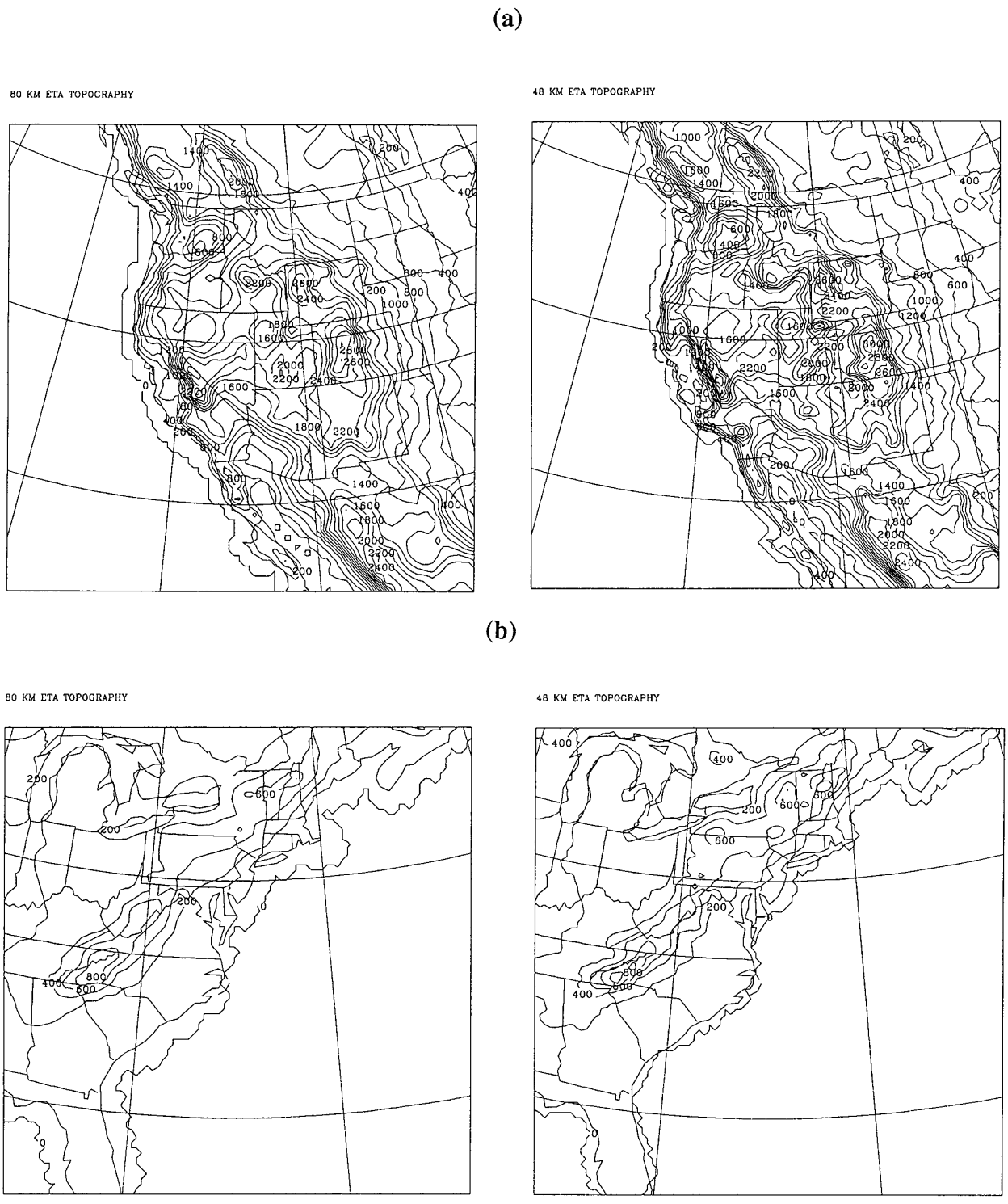

FIG. 2. Surface height for the 80- and 48-km eta model grids over (a) the western United States, (b) the eastern United States, and (c) Alaska. Contour interval = 200 m.

(c)

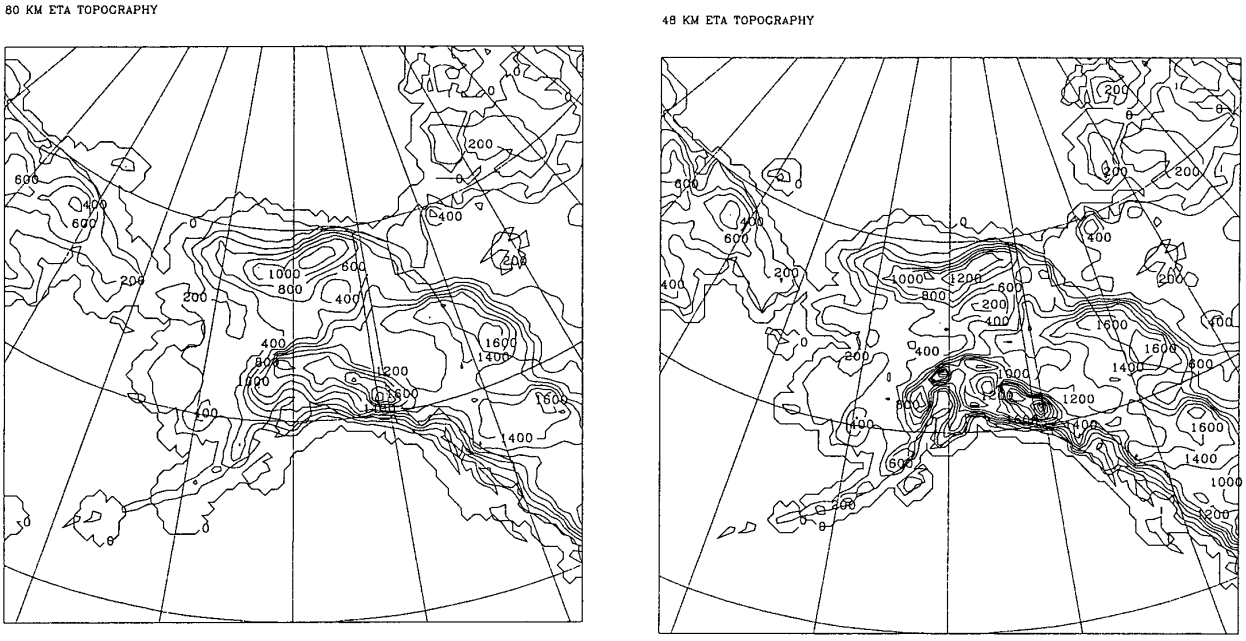

FIG. 2. (*Continued*)

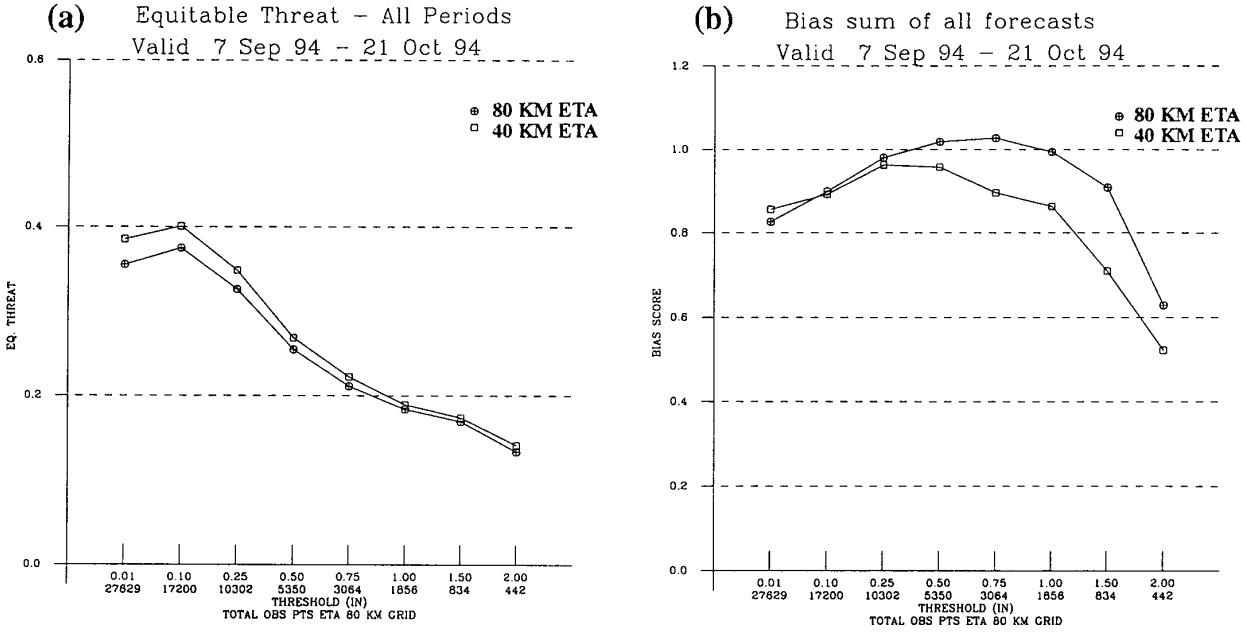

FIG. 3. (a) Equitable threat skill scores and (b) bias scores for 24-h precipitation forecasts (all periods) of the 80-km early eta and the 40-km eta model for the period 7 September–21 October 1994.

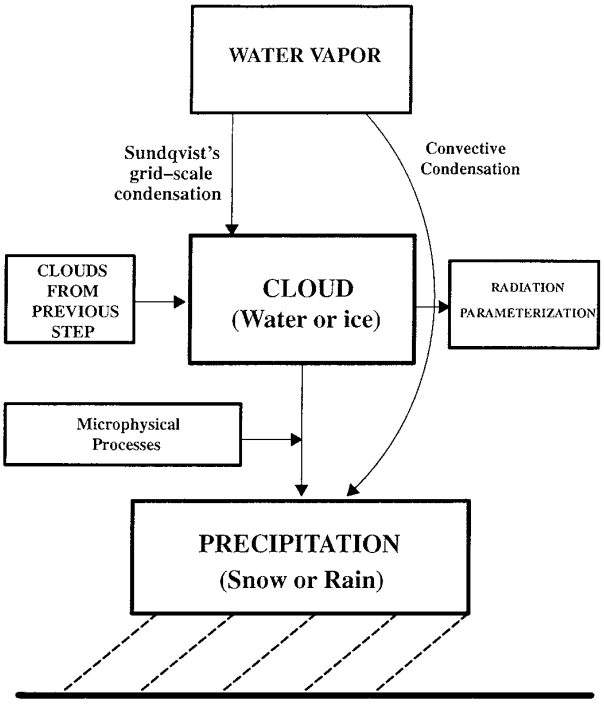

FIG. 4. Schematic illustration of the cloud prediction scheme.

at smaller grid spacings), efforts in developing prognostic schemes that explicitly predict cloud liquid water and ice have accelerated. Following the work of Sundqvist (1978) and Sundqvist et al. (1989), an increasing number of researchers have added cloud water and/or ice as a prognostic variable in their numerical models (Golding 1990; Pudykiewicz et al. 1992). Although computationally more expensive, the explicit prediction of cloud water allows for a more proper representation of the thermodynamic effects of condensation, as well as a more direct link between the radiative, dynamical, and hydrological processes in the model.

A cloud prediction scheme has been developed for the eta model (Zhao et al. 1995). One additional predictive variable, cloud water/ice mixing ratio, is used to represent combined cloud water and cloud ice in each layer of the model. A schematic overview of this scheme is given in Fig. 4. Water vapor is converted to cloud water/ice by grid-scale condensation (Sundqvist et al. 1989). Other physical processes such as evaporation, accretion of cloud water/ice to rain/snow, melting of snow, and autoconversion of cloud water/ice to precipitation are accounted for in the cloud scheme.

Figure 5 shows the distribution of cloud water and ice in a sample cloud as idealized by the cloud model. Cloud regions where the temperature (T) > 0°C consist entirely of cloud water, while clouds with $T < -15$°C contain only cloud ice. In the intermediate region, -15°C $< T < 0$°C, the phase of the hydrometeors is determined by the cloud-top temperature T_p. When T_p is > -15°C, the cloud consists of supercooled water. When T_p is < -15°C, the cloud consists of ice particles, based on the assumption that the cloud should freeze quickly because of the seeding effects of ice particles from above.

Based on the change of specific humidity and temperature predicted by the cloud scheme, a relative humidity is diagnosed at each model layer that is used to calculate a cloud fraction, b, defined as

$$b = 1 - \left(\frac{U_s - U}{U_s - U_{00}}\right)^{1/2} \quad \text{if } U > U_{00}$$

$$b = 0 \quad \text{if } U < U_{00}, \qquad (1)$$

where U is the relative humidity, $U_s = 1.0$ is the relative humidity in a cloud region, and U_{00} is the critical value of relative humidity for condensation. To avoid excessive condensation over water, U_{00} is set to 0.80 over ocean and 0.75 over land. The cloud fractions calculated using (1) are indirectly used in the model's radiation parameterization. Three layers of clouds (high: 350–150 mb, middle: 642–350 mb, and low: surface–642 mb) are calculated from the cloud fractions in each model layer, which are then provided to the radiation scheme.

The improvement in 40-km eta model forecasts of precipitation with the addition of the cloud model is evident from the equitable threat and bias scores of 24-h precipitation for September and October 1994 (Fig. 6). At all thresholds, the cloud scheme has improved the ETS of eta model precipitation forecasts. The inclusion of the cloud model tends to partially mitigate the underprediction of precipitation in the 40-km eta model (compare bias scores in Figs. 3 and 6) during the 6-week test period. According to Zhao et al. (1995), the inclusion of cloud water and ice above the freezing level, improved treatment of the evaporation of precipitation below cloud base, and the horizontal redistribution of cloud water/ice through advection processes are the factors contributing to improved precipitation scores.

Figure 7 shows the root-mean-square difference between rawinsonde observations (United States only) and the 24-h specific humidity forecasts from the 40-km eta model with and without the cloud scheme for September 1994. Small improvements in the moisture forecasts using the cloud scheme are seen at levels below 800 mb and above 550 mb. A similar trend is observed in the bias (forecast–observation, not shown). The cloud scheme accounts for both condensation onto liquid water droplets and deposition onto ice particles, which probably accounts for the improvements in the upper-level moisture forecasts. The positive impact near the surface reflects the effect of the improved parameterization of the large-scale condensation of

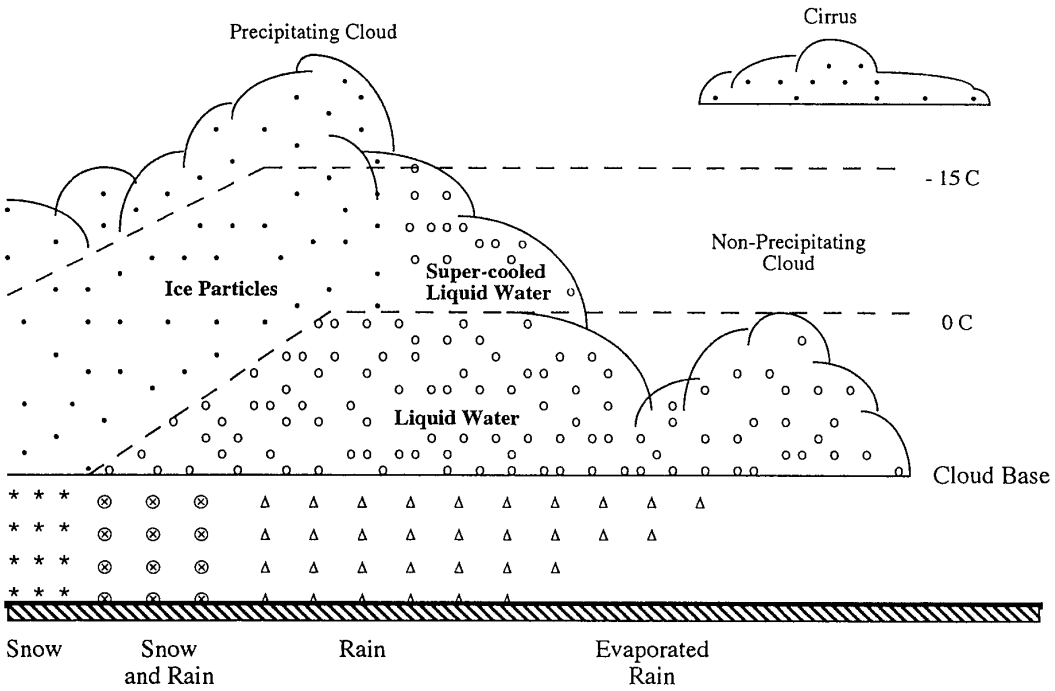

FIG. 5. Distribution of cloud water and cloud ice in the cloud prediction scheme.

clouds and the treatment of evaporating precipitation below cloud base.

Although the cloud model has a positive impact on precipitation and specific humidity forecasts, the impact on the temperature forecasts was minimal in September 1994 (not shown). The reasons for this are not clear. We hypothesize that the partitioning of the individual model-layer cloud fractions produced by the

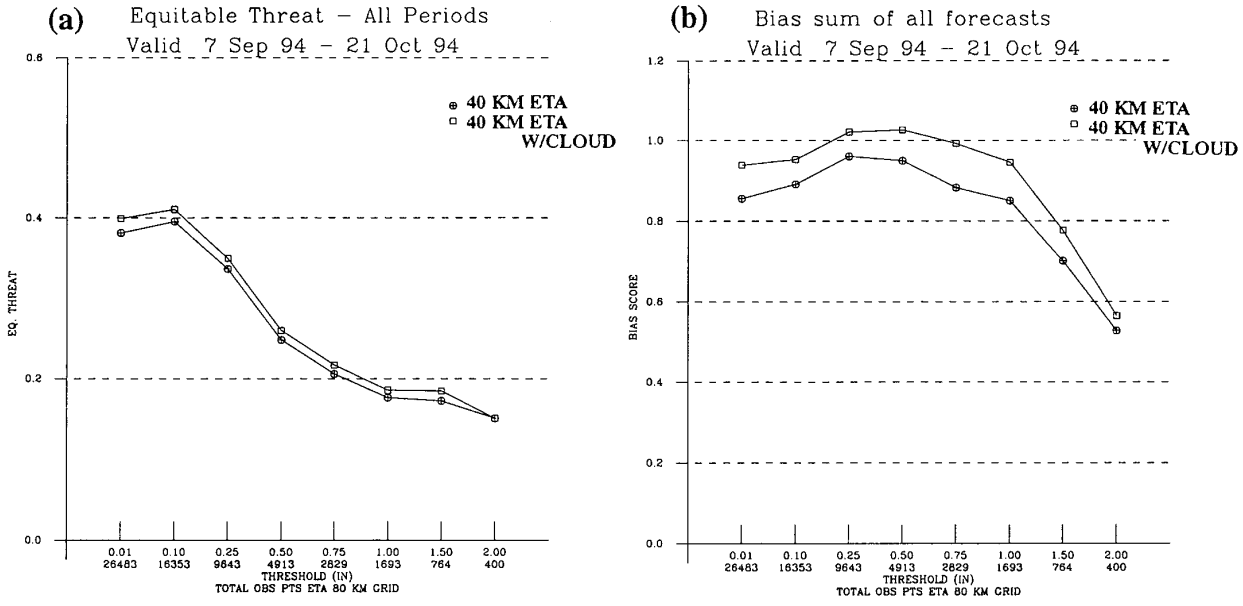

FIG. 6. As in Fig. 3 but for the 40-km eta model without cloud water and the 40-km eta model with cloud water.

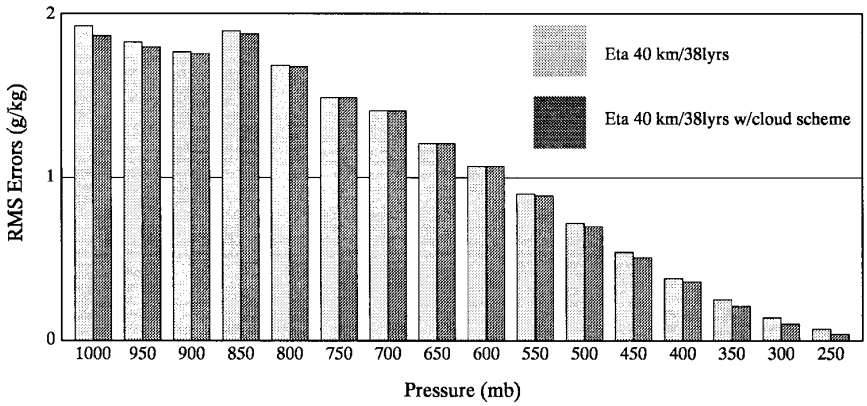

FIG. 7. Root-mean-square errors of the 24-h specific humidity forecasts at pressure levels from the 40-km eta model with and without the cloud scheme for September 1994.

cloud model into low, middle, and high cloud fractions may reduce the impact of the predicted cloud on the radiative adjustments to temperature in the model. This problem will be revisited when the eta model's radiation parameterization is changed to allow direct use of the cloud fraction in each model layer.

c. The Eta Data Assimilation System

To ensure the most accurate prediction possible, it is important to produce initial conditions that are consistent with the forecast model. If data assimilation is performed using a regional model, the initial conditions

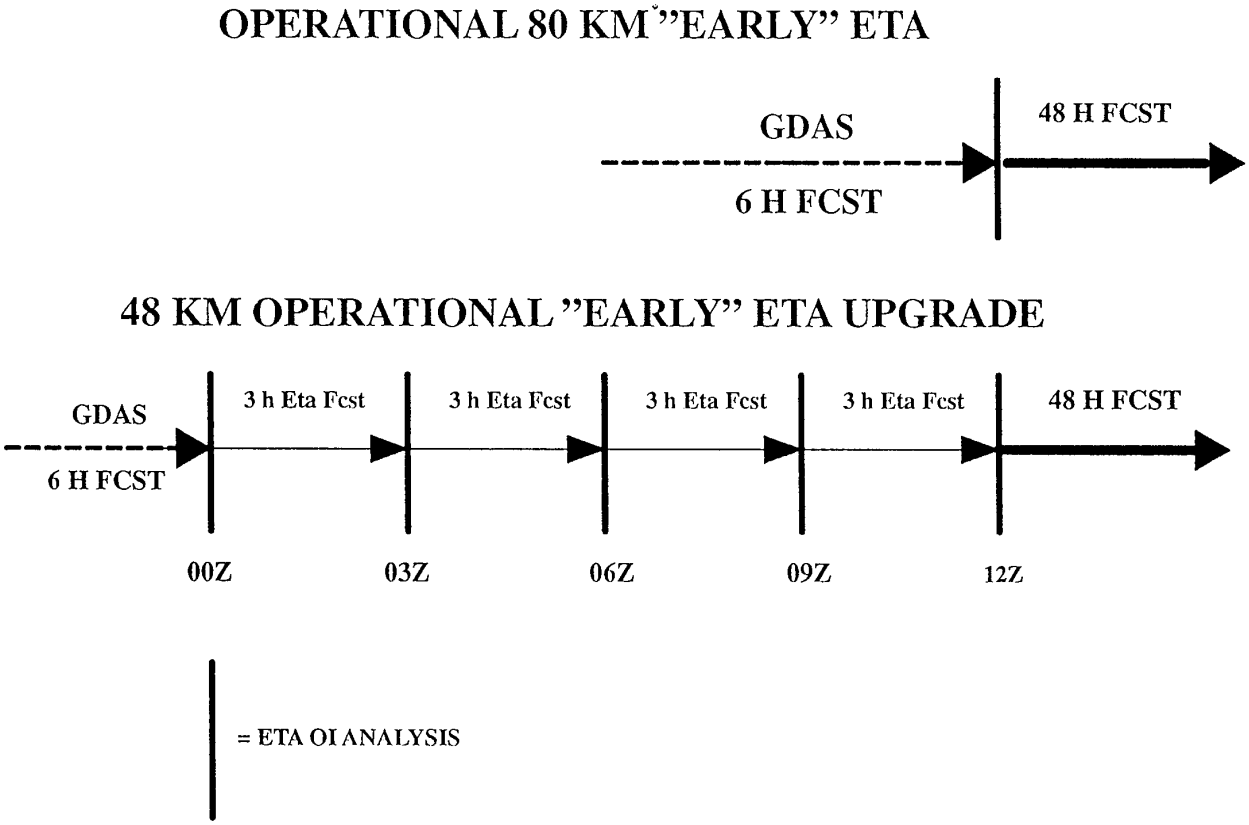

FIG. 8. Schematic representation of the analysis systems for the 80-km early eta and the 48-km early eta upgrade.

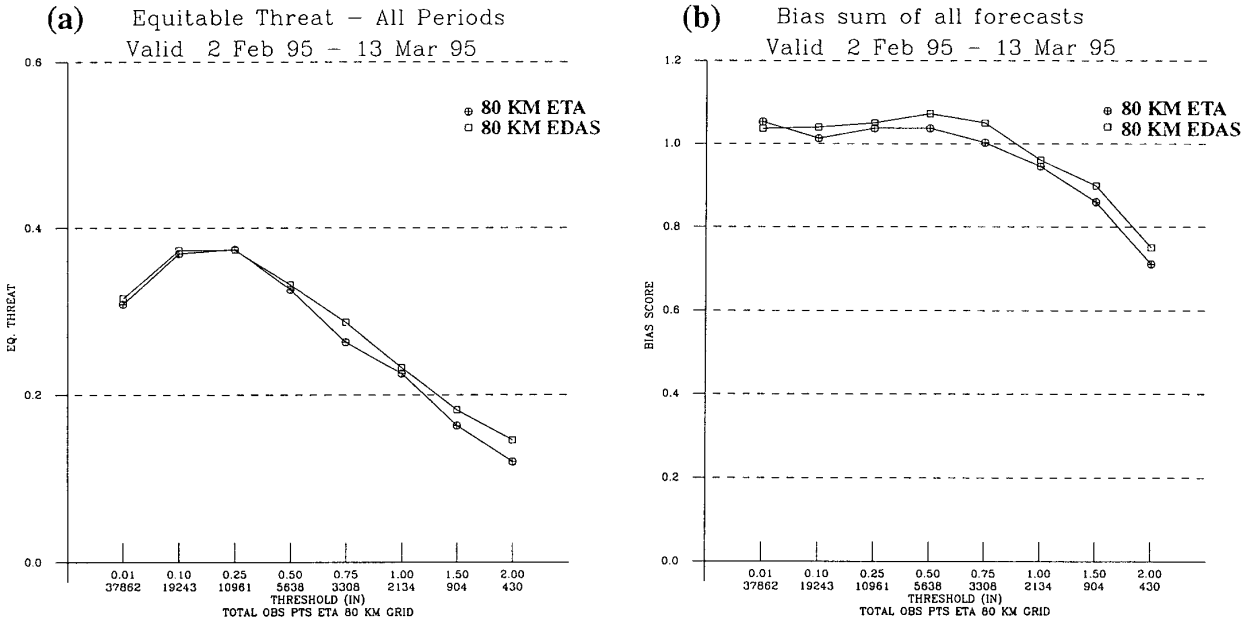

FIG. 9. As in Fig. 3 but for the 80-km early eta and the 80-km EDAS forecasts for the period 2 February–13 March 1995.

will better reflect the resolution, physics, and dynamics of the regional model than would a global model with lower resolution and different physical parameterizations. For these reasons NCEP has developed an intermittent data assimilation system using the eta model.

The Eta Data Assimilation System (EDAS) is analogous to the intermittent Regional Data Assimilation System (DiMego et al. 1992), which is used to initialize the Nested Grid Model (NGM). A schematic depiction of the 48-km EDAS and the previous 80-km early eta analysis system is presented in Fig. 8. The 80-km early eta was started with a first guess valid at 0000/1200 UTC (T00), obtained from a 6-h global forecast from the GDAS. The NCEP global spectral model, the forecast component of the GDAS, is currently configured at T126 resolution (~105 km) with 28 sigma layers. The data processing and ROI analysis used in the 80-km early eta system were described in Black et al. (1993) and Rogers et al. (1995).

The EDAS employs the same ROI analysis as was used in the September 1994 version of 80-km early eta as described by Rogers et al. (1995), except than the analysis is done directly on the 48-km grid. The major advantage of the EDAS, as illustrated in Fig. 8, is that after the GDAS is used to start the assimilation at 12-h prior to model start time, the eta model is used to assimilate the observations at 3-h intervals throughout the 12-h preforecast assimilation period. The 3-h analysis updates in the EDAS allow for the use of high-frequency observations, such as wind profiler, WSR-88D, and aircraft data, in a more timely manner than does the 6-h analysis cycle in the GDAS. The use of the higher-resolution eta model during the assimilation should produce a more consistent first guess for the eta ROI analysis than that obtained from the NCEP global spectral model.

The impact of the EDAS on precipitation skill scores is shown in Fig. 9. During February and March 1995 an 80-km version of the EDAS and accompanying 48-h eta model forecast were run in parallel to the 80-km early eta. The version of the model used in this test did not include the cloud scheme described in section 2b. Thus, the differences in precipitation scores are caused solely by the use of the EDAS to initialize the model. The EDAS-based forecasts had slightly higher ETS than the early eta forecasts, while the bias scores show that the 80-km EDAS forecast more precipitation than the 80-km early eta at all thresholds except rain/no rain. The equitable threat and bias scores for the individual 0- to 24-h, 12- to 36-h, and 24- to 48-h forecasts (not shown) reveal a similar signal.

Figures 10a and 10b show the observed temperature and the 80-km early eta initial postprocessed 2-m (shelter height) temperature, respectively, at 1200 UTC 9 February 1994. The observed temperature field depicts a typical cold season pattern over the mid-Atlantic states, with cold air dammed up east of the Appalachian mountains over Maryland, eastern Virginia, and southwestern Pennsylvania. The 80-km early eta analysis failed to capture this cool pool of air, with errors as high as 10°C. The analysis from

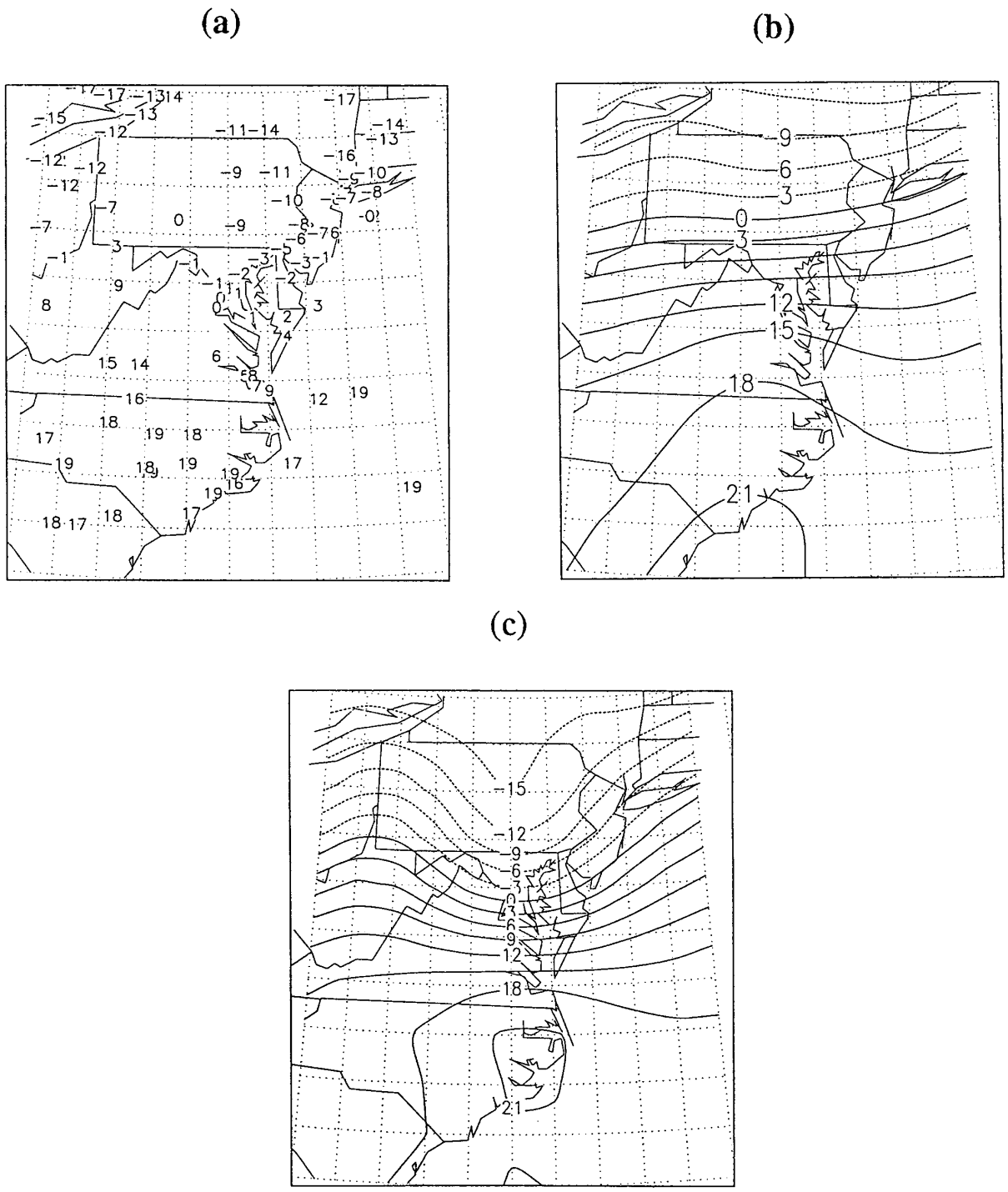

FIG. 10. (a) Observed surface temperatures (°C) at 1200 UTC 9 February 1994. (b) Postprocessed 2-m (shelter) temperatures (°C) from the early eta analysis valid at 1200 UTC 9 February 1994. Contour interval = 3°C. (c) As in (b) but for the 80-km EDAS analysis.

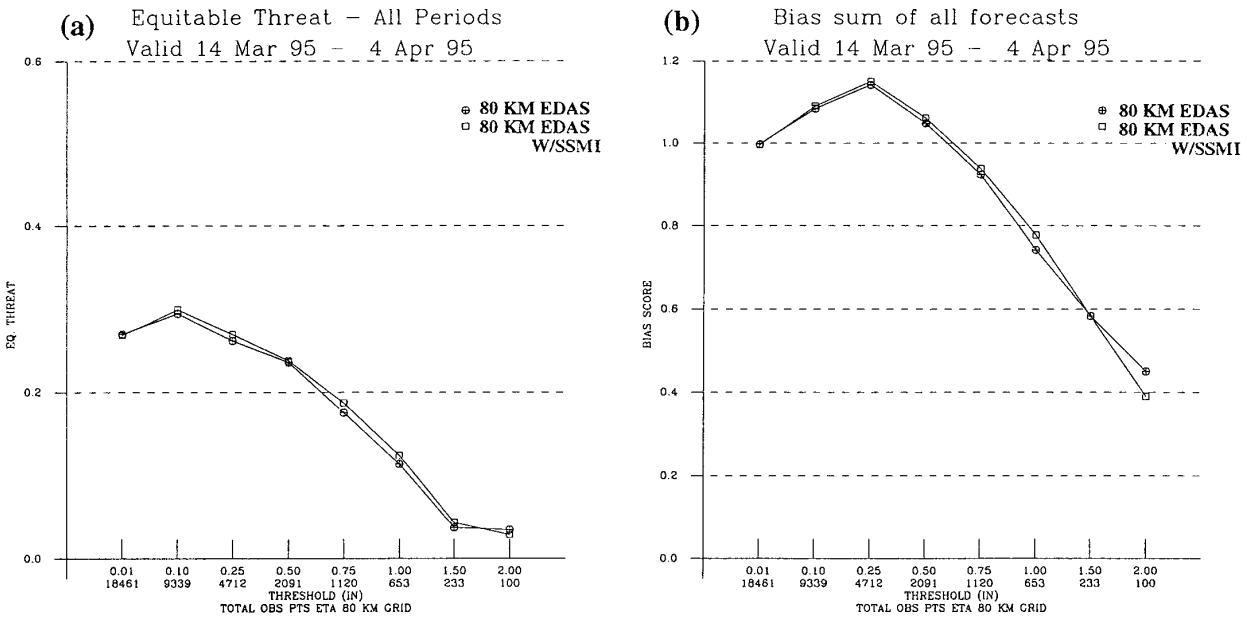

FIG. 11. As in Fig. 3 but for forecasts from the 80-km EDAS and the 80-km EDAS with SSM/I total column water data for the period 13 March–3 April 1995.

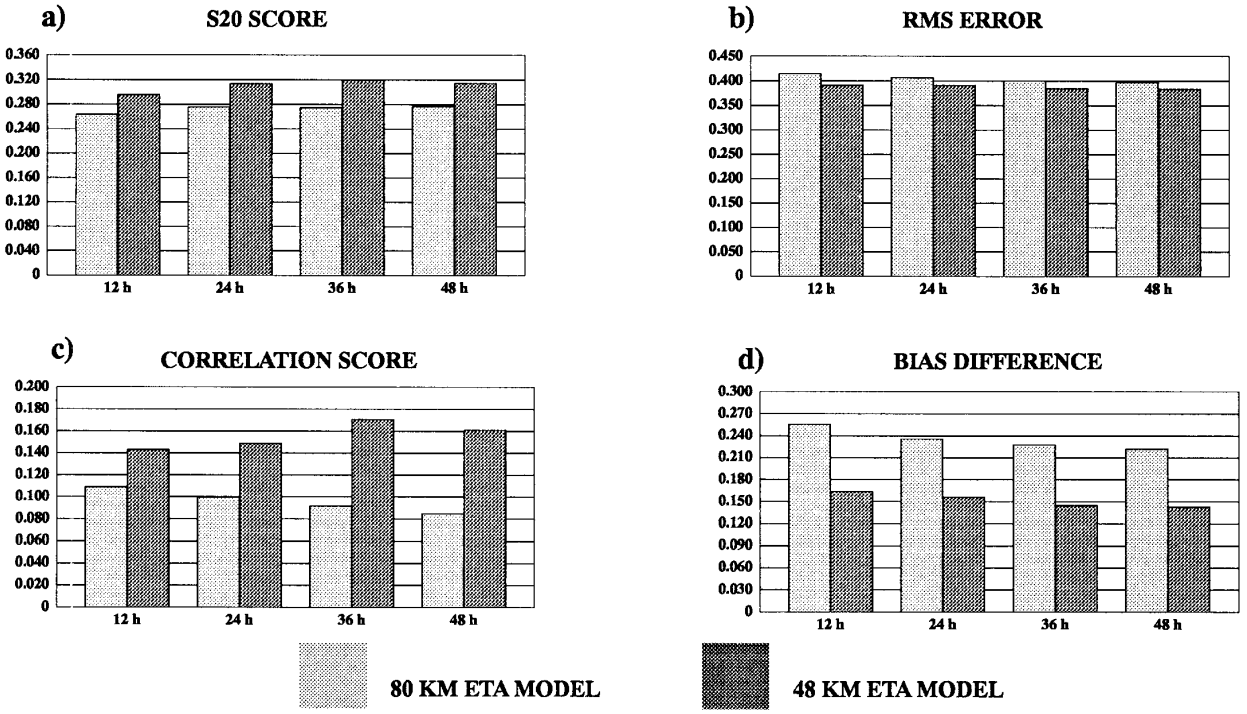

FIG. 12. (a) S20 score, (b) rms error score, (c) correlation score, and (d) bias difference score of the total cloud fraction from the 80-km early eta (light) and the 48-km eta model (dark) for the period 9–16 March 1995.

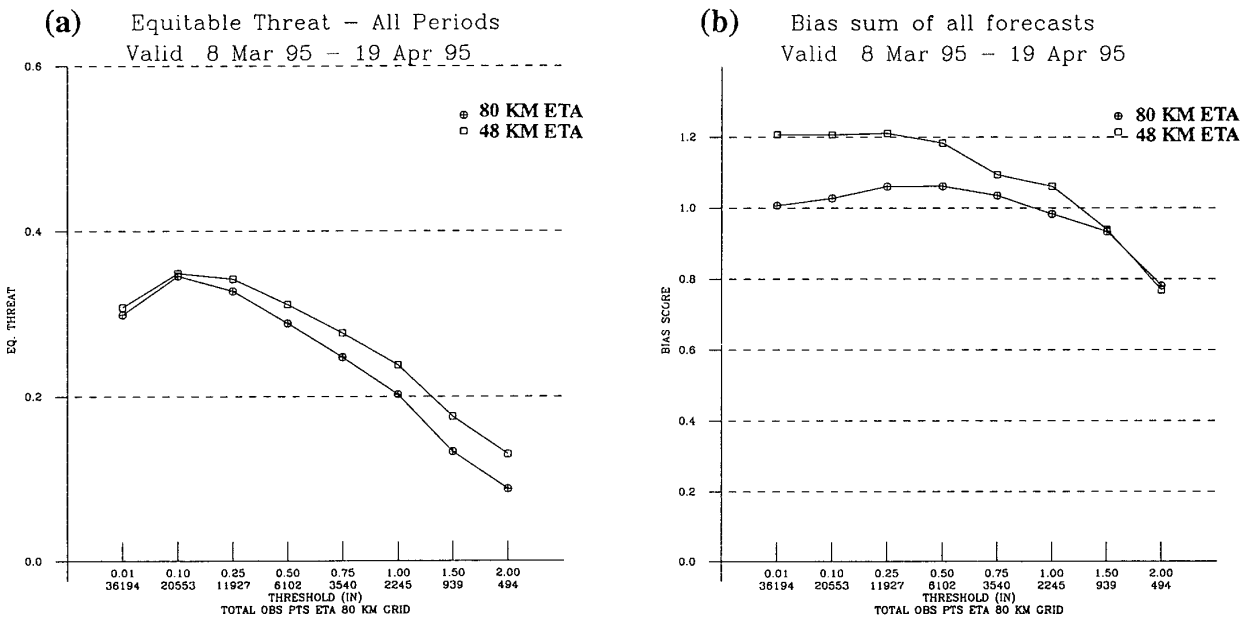

FIG. 13. As in Fig. 3 but for the 80-km early eta and the 48-km eta model forecasts for the period 7 March–18 April 1995.

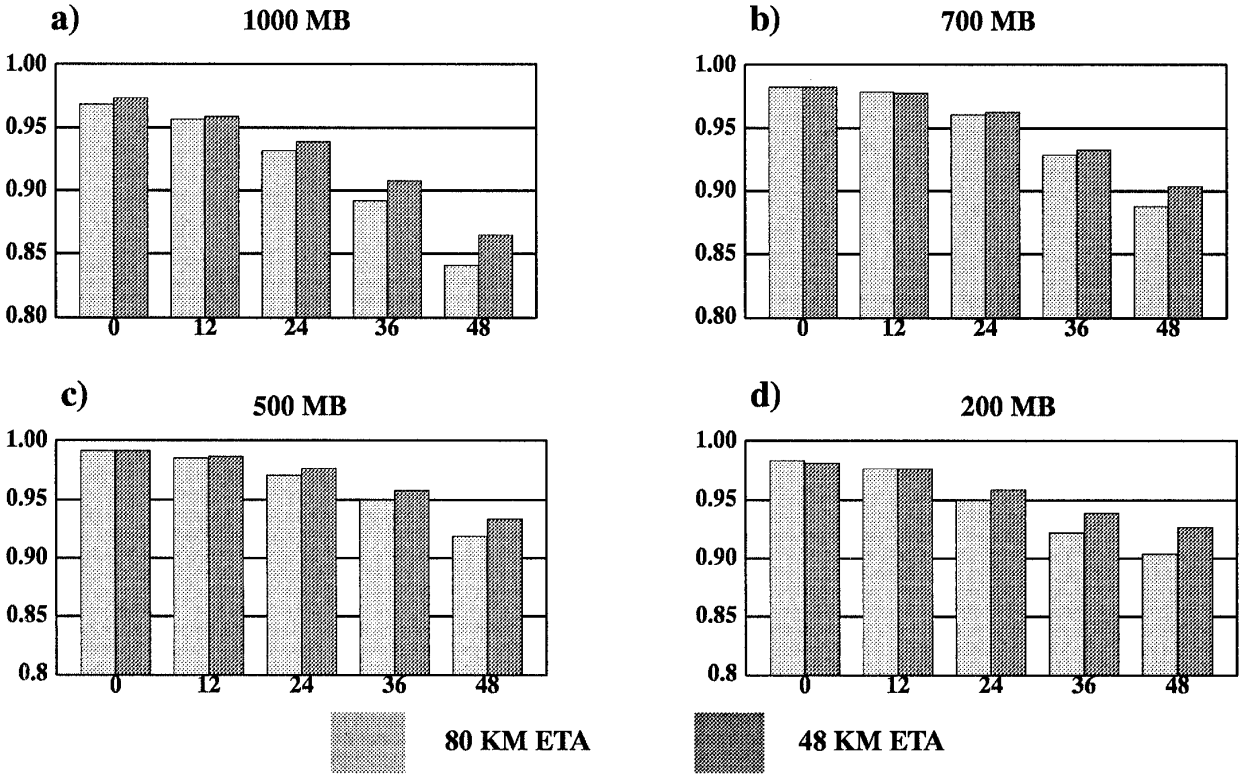

FIG. 14. Anomaly correlation coefficient for height at (a) 1000, (b) 700, (c) 500, and (d) 200 mb for 0-, 12-, 24-, 36-, and 48-h forecasts for the 80-km early eta (light) and the 48-km eta model (dark) computed over all NGM D grid land points for the period 5–16 April 1995. RAFS analysis is used as truth.

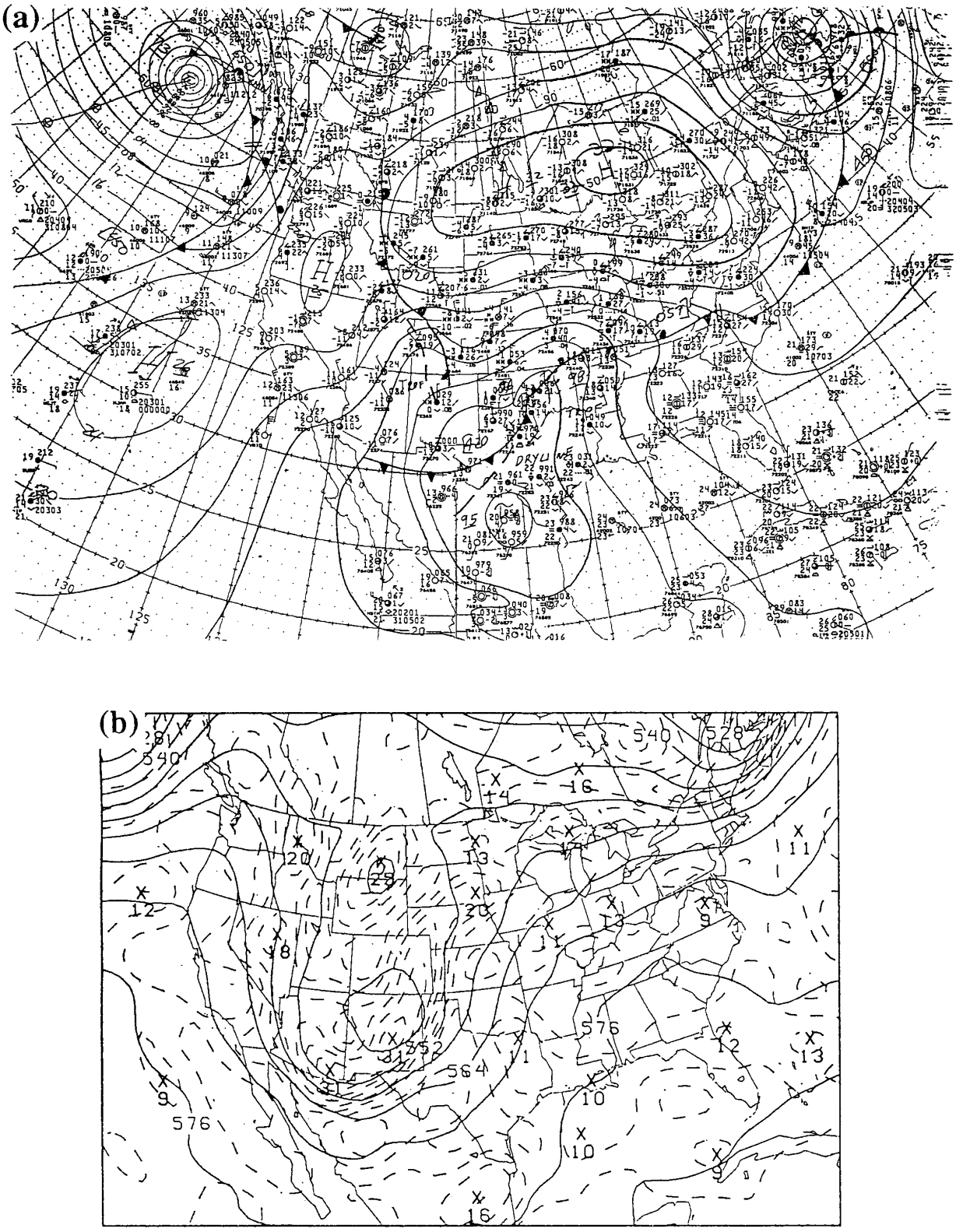

FIG. 15. (a) NCEP mean sea level pressure (mb) analysis valid at 1200 UTC 10 April 1995. (b) The 80-km early eta 500-mb height analysis (dam) and 500-mb absolute vorticity (10^{-5} s^{-1}) valid at 1200 UTC 10 April 1995.

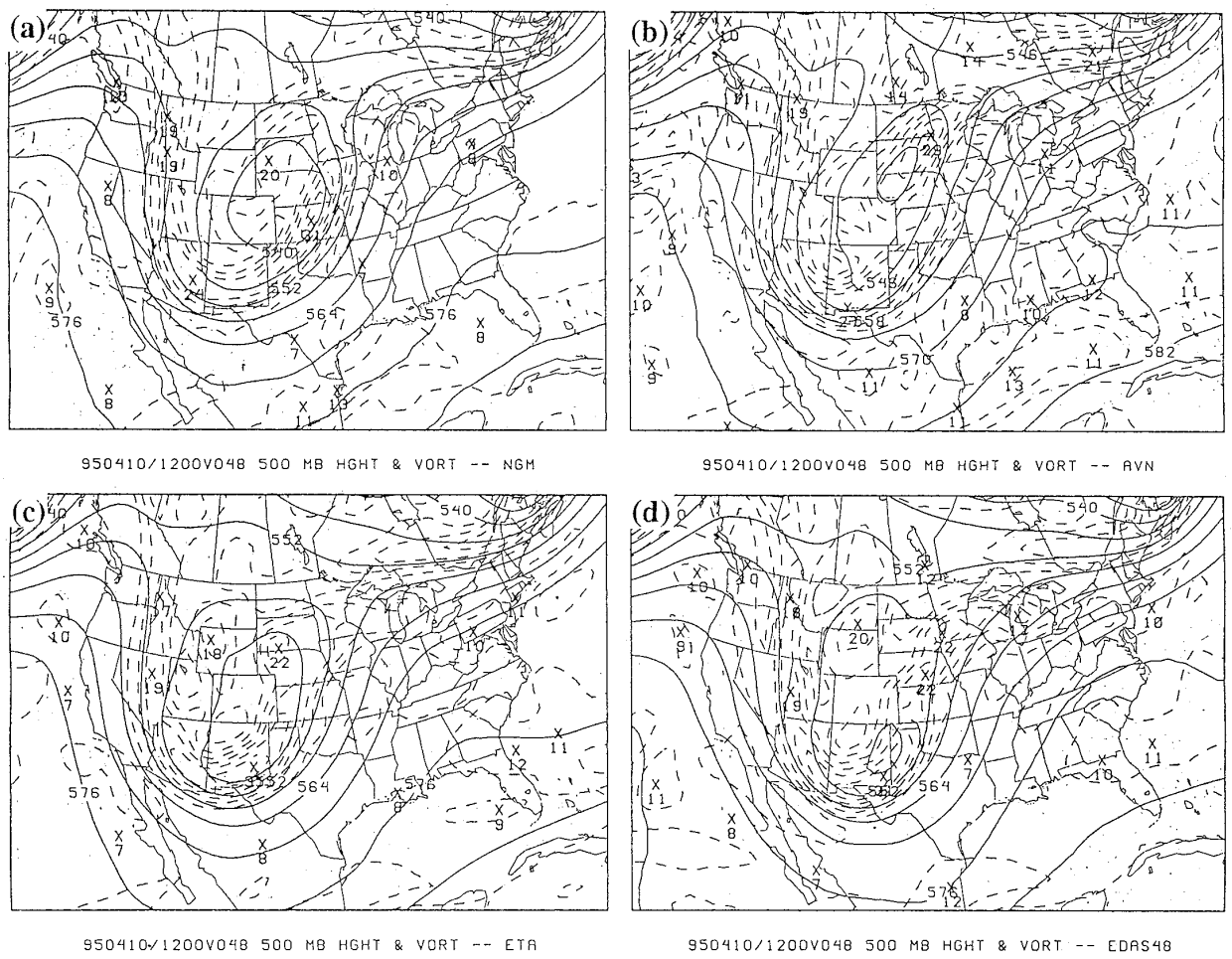

FIG. 16. The 48-h forecasts of 500-mb heights (dam) and absolute vorticity (10^{-5} s^{-1}) valid at 1200 UTC 10 April 1995 from (a) the NGM, (b) the aviation run of the NCEP global spectral model (AVN), (c) the 80-km early eta, and (d) the 48-km eta model.

an 80-km EDAS run (Fig. 10c) is more realistic, capturing the essential features of the cool pool, although significant details such as the southern extension of the cold air toward Richmond, Virginia, were still missed.

d. Satellite moisture observations

To improve the initialization of moisture in its numerical models, NCEP must rely on remotely sensed observations, especially over oceanic regions where rawinsonde reports are sparse. In the past, NCEP has used subjective vertical moisture profiles derived from cloud imagery over the oceans. Currently, efforts are under way at NCEP to develop techniques to assimilate moisture information sensed directly by satellites. One such source that has been tested in the eta model analysis system is vertically integrated water vapor (IWV) measured by the Special Sensor Microwave/Imager (SSM/I) on board the polar-orbiting Defense Meteorological Satellite Program satellites (Alishouse et al. 1990).

SSM/I IWV data are converted into vertical moisture profiles for use by the eta ROI analysis using a technique developed by Lin et al. (1995). At each IWV observation location, the first-guess specific humidity field is interpolated to the IWV data point, from which the first guess IWV is calculated. The ''SSM/I'' moisture profile is obtained by multiplying the first-guess specific humidity profile by the ratio IWV_{obs}/IWV_{guess}. Specific humidity increments are obtained by differencing the SSM/I moisture profile and the first-guess moisture profile. These increments are input into the eta ROI univariate specific humidity analysis.

An experiment using the SSM/I IWV data in an 80-km EDAS system was performed during March and April 1995. Control for this test was the 80-km EDAS system described in section 2c, which was run without

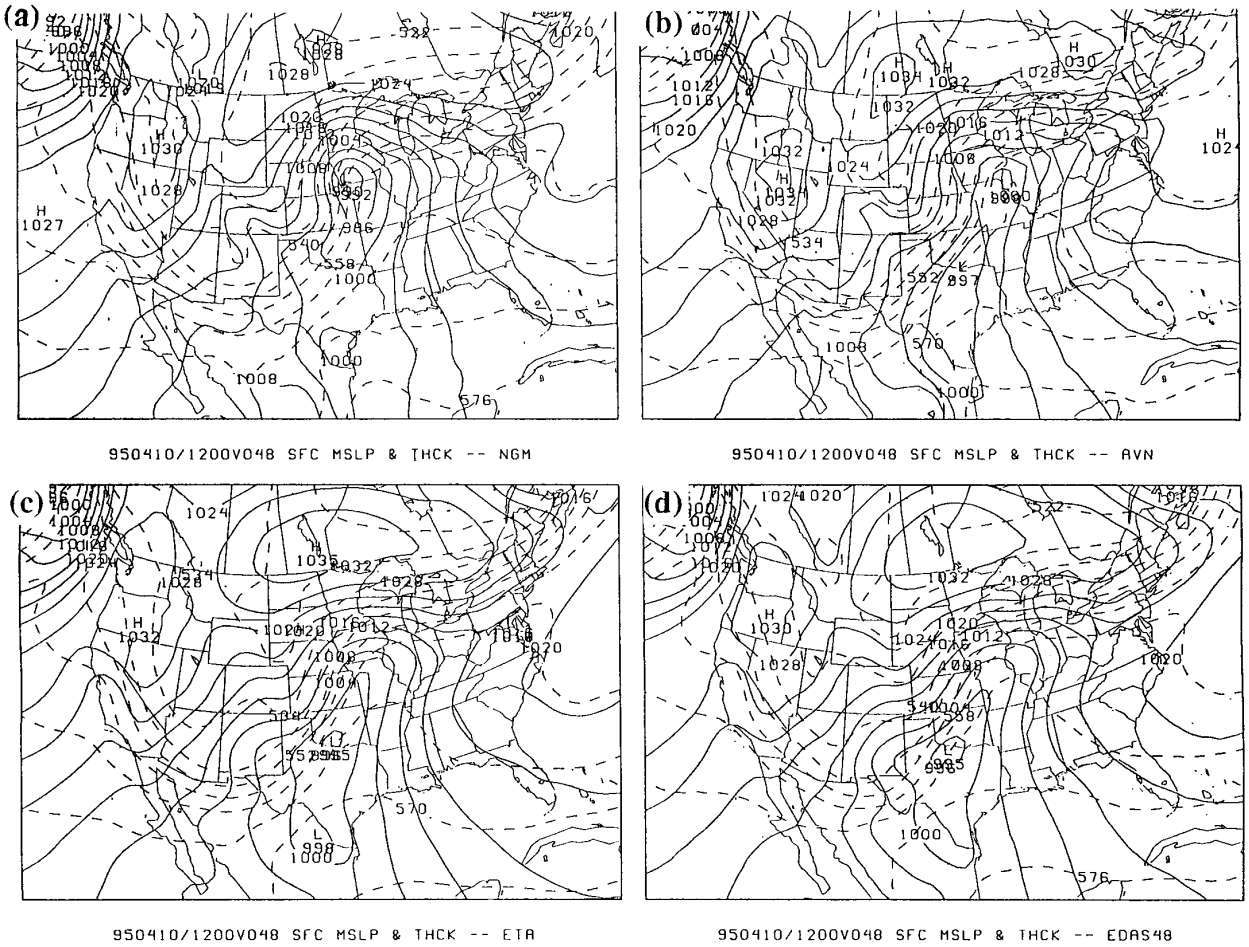

FIG. 17. As in Fig. 16 but for mean sea level pressure (mb) and 1000–500-mb thickness (dam).

the SSM/I data. Although the IWV data is retrieved only over the ocean, the ETS and bias scores from the forecasts with the SSM/I data were equal to or higher than the control run at all but the 2.0-in. threshold (Fig. 11). Additionally, results from a test of these data in a static eta ROI system during October–November 1994 (not shown) indicate that in some instances the use of the SSM/I IWV data in the eta ROI analysis improved the simulation of convective precipitation in the tropical oceans, using satellite-based estimates of convective rainfall as truth. Based on these findings, the SSM/I IWV data have been used in the upgraded early eta system since it was operationally implemented in October 1995.

3. Verification results

a. Objective scores

1) TOTAL CLOUD COVERAGE

Quantitative verification of total cloud coverage for the 80-km early eta and the 48-km upgrade was performed using real-time 3-h nephanalyses produced by the Air Force Global Weather Center (AFGWC; Hamill et al. 1992). While the cloud coverage from the 48-km model is based on the direct prediction of clouds in the model, the clouds from the 80-km early eta are diagnosed from the model's forecast of relative humidity and convective rainfall rate, generally following the method described by Slingo (1987). After the AFGWC cloud analysis is interpolated to the eta model grid, four statistical scores are computed: S20 score (the percent of points where the cloud amounts between the forecast and observed differ by less than 20%), correlation score, rms difference score, and the bias. Higher S20 and correlation scores and lower rms difference indicate a better forecast, as do bias scores closer to unity. These scores for the 80-km early eta and 48-km eta model for 9–16 March 1995 are presented in Fig. 12. For all forecast periods, the prognostic clouds from the 48-km eta model are closer to the nephanalysis than the clouds diagnosed from the early eta forecast. A previously observed ''spinup'' in the prognostic clouds in

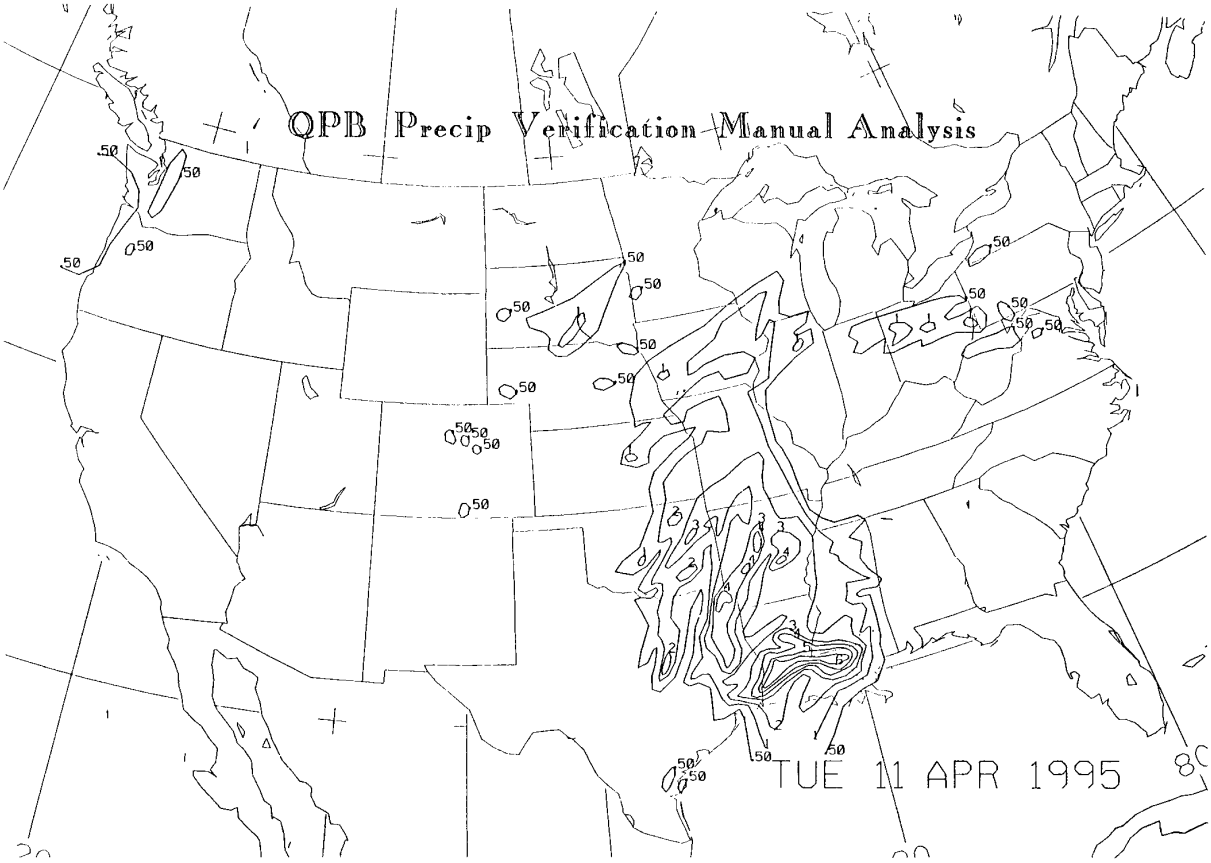

FIG. 18. Subjective analysis of 24-h accumulated precipitation amount (in) valid at 1200 UTC 11 April 1995 from the Quantitative Precipitation Branch of the Hydrometeorological Prediction Center of NCEP.

an experiment with a 40-km eta model using a static ROI analysis (Zhao et al. 1995; not shown) is not seen in the bias scores from the 48-km model, which is better than the 80-km model at 12 h. The use of the EDAS with the cloud prediction scheme in the assimilating model may have been responsible for the absence of this spinup problem in the 48-km eta forecast.

2) PRECIPITATION

Figure 13 shows the equitable threat and bias scores of 24-h accumulated precipitation over the contiguous United States from the 80-km early eta and the upgraded 48-km system for March–April 1995. At all thresholds the 48-km forecasts attained better ETSs than the early eta forecasts, with the greatest improvement seen at the thresholds above 1 in. The use of both the EDAS and the cloud scheme has eliminated the underprediction of precipitation seen in the previous higher-resolution eta model forecasts (Fig. 3). The 48-km upgrade package actually overpredicted 24-h precipitation at thresholds below 1 in. This may indicate that further tuning of the cloud scheme at 48-km grid spacing is needed.

3) FORECAST VERSUS ANALYSIS VERIFICATION–ANOMALY CORRELATION

Verification of the 80-km early eta and the 48-km eta model forecasts has been performed using the analyses from the NCEP Regional Analysis and Forecast System (RAFS; Hoke et al. 1989) as truth. All model and verification fields are interpolated from their respective grids onto NCEP Office Note 84 (U.S. Dept. of Commerce 1994) grid 107, the so-called NGM D grid. This grid is exactly one-half the grid spacing ($\sim$40 km) of the innermost computational grid of the NGM. Verifications were performed only for the North American land points of the D grid, and summed quantities were weighted by the inverse map-scale factor (proportional to area).

Figure 14 shows the anomaly correlation (AC) for geopotential height forecasts from the 80-km early eta and 48-km eta model for 5–16 April 1995 at 1000, 700,

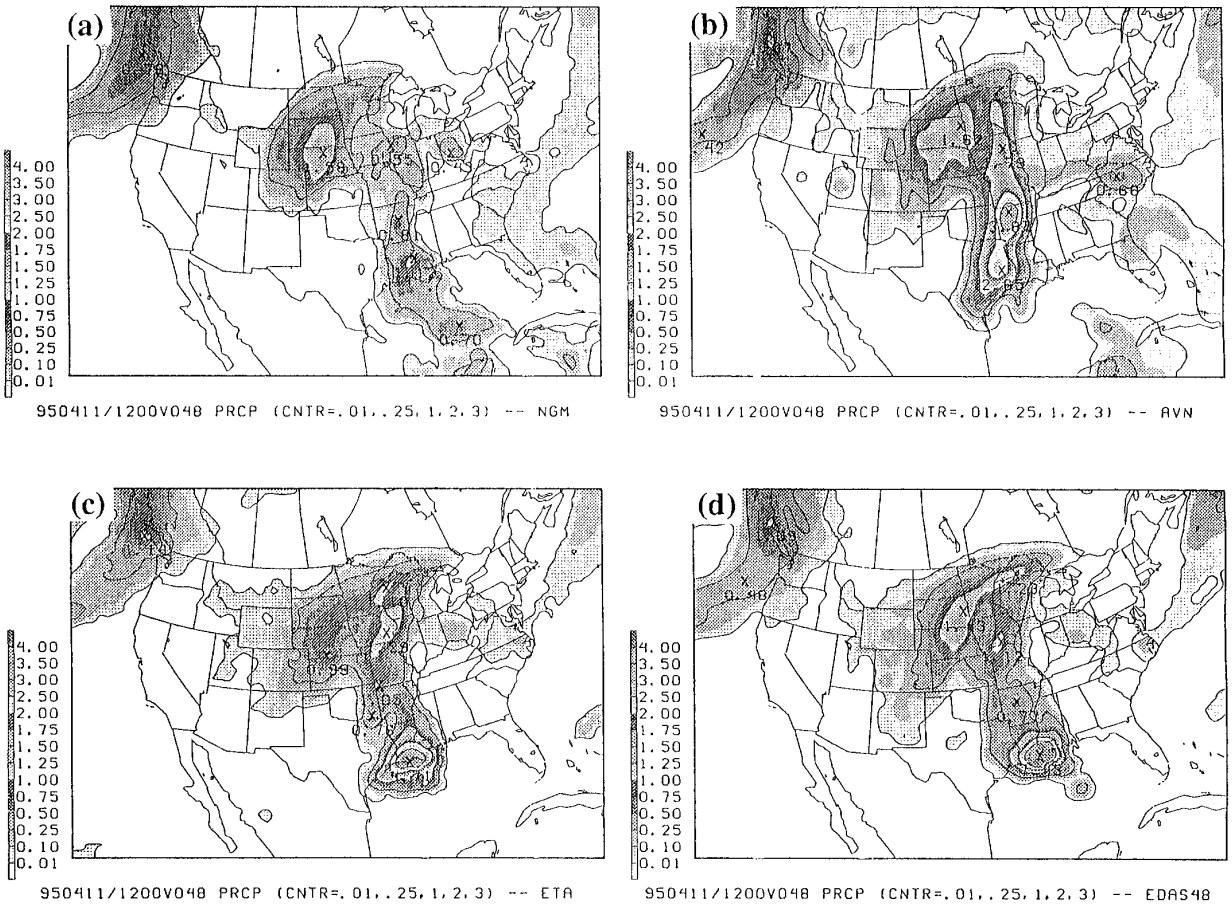

FIG. 19. The 48-h forecasts of 24-h accumulated precipitation amount (in.) valid at 1200 UTC 11 April 1995 from (a) the NGM, (b) the aviation run of the NCEP global spectral model (AVN), (c) the 80-km early eta, and (d) the 48-km eta model. Contouring/shading of precipitation shown to the left of each figure.

500, and 200 mb. This score is the correlation between the forecast departure and observed departure from climatology. A perfect forecast (AC = 1) would reproduce the observed anomaly (analysis minus climatology). The RAFS analyses were used to compute the observed anomaly. Figure 14 reveals that the 48-km model consistently scores higher than the 80-km early eta at all levels and at all forecast times. The greatest improvement is seen in the latter half of the forecast at 200 mb.

b. Subjective evaluation

A subjective evaluation of 48-km eta model forecasts against the 80-km early eta, the NGM, and the aviation run of the NCEP global spectral model (AVN) was performed during an 18-day period in April 1995. This evaluation stressed the ability of each model to accurately predict precipitation and the movement and intensity of weather systems across the United States.

In general, both the 48- and 80-km eta models forecast cyclone movement from the Rockies into the Great Plains more accurately than either the NGM or the AVN. The NGM and the AVN characteristically predict surface cyclones to track too far north across the Great Plains, leading to forecasts of 500-mb heights that are lower than observed over the northern Great Plains. An example that shows how much better the two eta models can predict these storms is depicted in Figs. 15–17. Figure 15 shows the NCEP sea level pressure analysis and the early eta analysis of 500-mb height analysis valid at 1200 UTC 10 April 1995. Figures 16 and 17 show the 48-h forecasts of 500-mb heights and sea level pressures, respectively, from the four models. In this case the NGM and AVN 500-mb height forecasts were ~120 m too low over central South Dakota (Figs. 16a and 16b). Additionally, these models placed the surface low well to

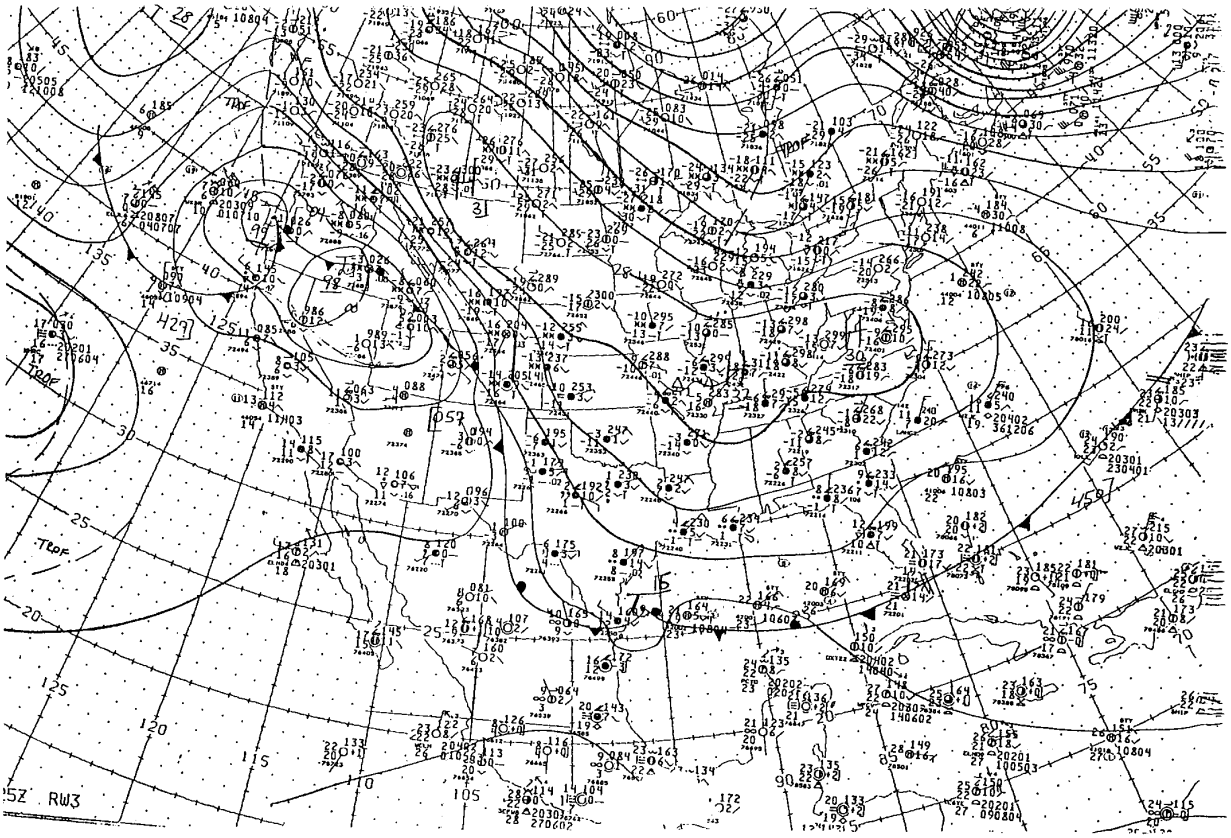

FIG. 20. NCEP mean sea level pressure (mb) analysis valid 1200 UTC 13 February 1995.

the north of its observed position in Oklahoma (Fig. 17). The 48 and 80-km eta models, by contrast, predicted a much weaker cyclone that was much closer to the observed location.

During the April 1995 evaluation, both versions of the eta model appeared to more accurately forecast the location of east–west frontal bands located east of the Mississippi River, by placing the fronts farther to the south than either the NGM or AVN. The 48-km eta model's skill at predicting the strength and location of surface lows appears to be comparable to that of the 80-km early eta. The 48-km eta model, however, appeared to be better than the 80-km early eta at predicting the pressures of filling cyclones.

The 48-km eta system was clearly the best model in predicting precipitation during a subjective evaluation of 27 forecasts during April 1995. During the period, the 48-km eta model was judged the best model 17 times compared to 7 times for the 80-km early eta. An example of an improved precipitation forecast from the 48-km eta model is shown in Figs. 18–19. Figure 18 shows the NCEP manual analysis of 24-h precipitation valid at 1200 UTC 11 April 1995. During the previous 24-h period very heavy rain fell over parts of Louisiana, with an analyzed maximum of 6 in. Individual stations in this area reported amounts up to 11 ins. The 24–48-h precipitation forecasts valid at 1200 UTC 11 April 1995 (Fig. 19) from the four models shows that the 48-km eta model did a remarkable job predicting a major mesoscale heavy rainfall event over Louisiana. The 48-km eta model (Fig. 19d) forecast of over 7 in. of precipitation in Louisiana is clearly the best of the four models.

In general, the 48-km eta model appeared to be significantly better in forecasting convective precipitation across the gulf states and the Tennessee River Valley than any of the lower-resolution models, especially the NGM. The three operational models and the 48-km eta model appeared to overpredict the areal coverage of the amounts > 1 in. to the north of cyclones over the northern Great Plains during the period of study. In the western United States, the 48-km eta model appeared to capture the mesoscale precipitation patterns better than any of the other models. Despite its ability to better forecast convective precipitation in the southern United States, in two instances the 48-km eta model was pre-

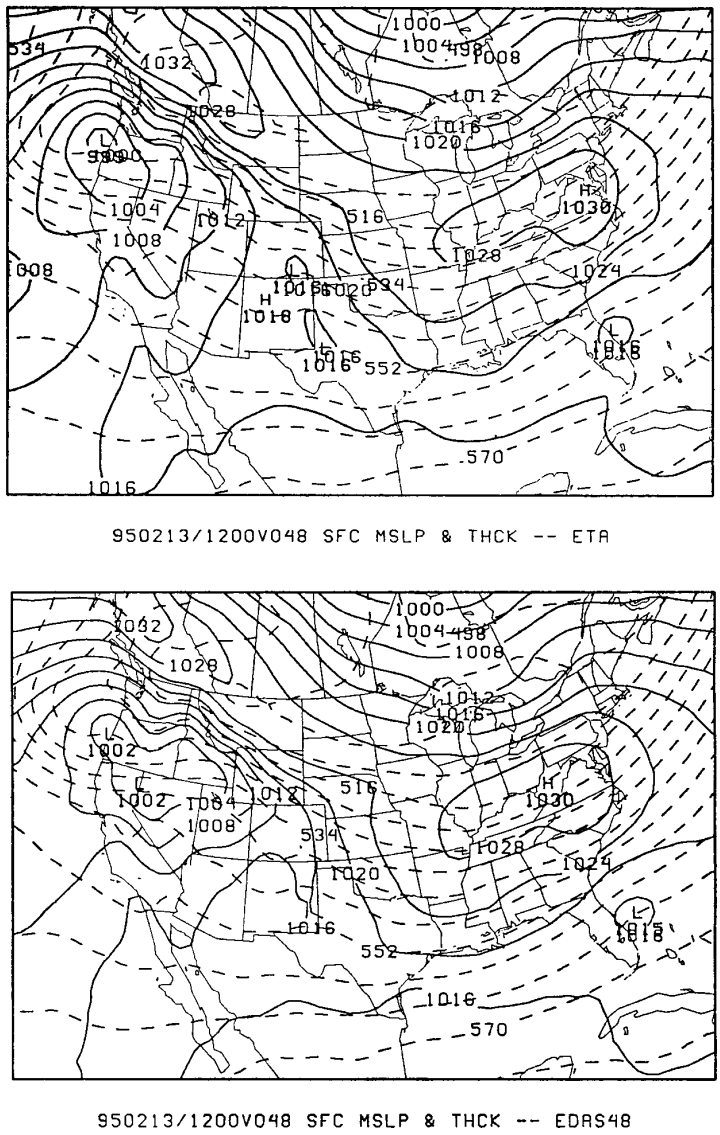

FIG. 21. The 48-h forecasts of mean sea level pressure (mb) and 1000–500-mb thickness (dam) valid at 1200 UTC 13 February 1995 from (a) the 80-km early eta (top) and (b) the 48-km eta model (bottom).

mature in forecasting precipitation over states bordering the Gulf of Mexico in advance of a cold front.

c. Forecast example: 13–15 February 1995

Figure 20 shows the NCEP analyzed mean sea level pressure valid at 1200 UTC 13 February 1995. The feature of interest is the cyclone just off the Oregon coast, which resulted in a significant snowfall in the Portland, Oregon, and Seattle, Washington, metropolitan areas. A trough of low pressure extends southeastward along a quasi-stationary front, with pressures below 1004 mb extending as far east as Utah. The 48-h forecasts valid at this time from the 80-km early eta and a parallel test of the full 48-km upgrade package are presented in Fig. 21. Although the precipitation forecasts were similar (not shown), the sea level pressure forecasts are different. The 80-km forecast more accurately predicted the strength of the coastal cyclone, but the 48-km forecast gave a better depiction of the frontal boundary and low pressure trough extending into Nevada and Utah.

By 1200 UTC 15 February 1995 (Fig. 22), the cyclone had reorganized east of the Rocky Mountains and was located over eastern Minnesota, with

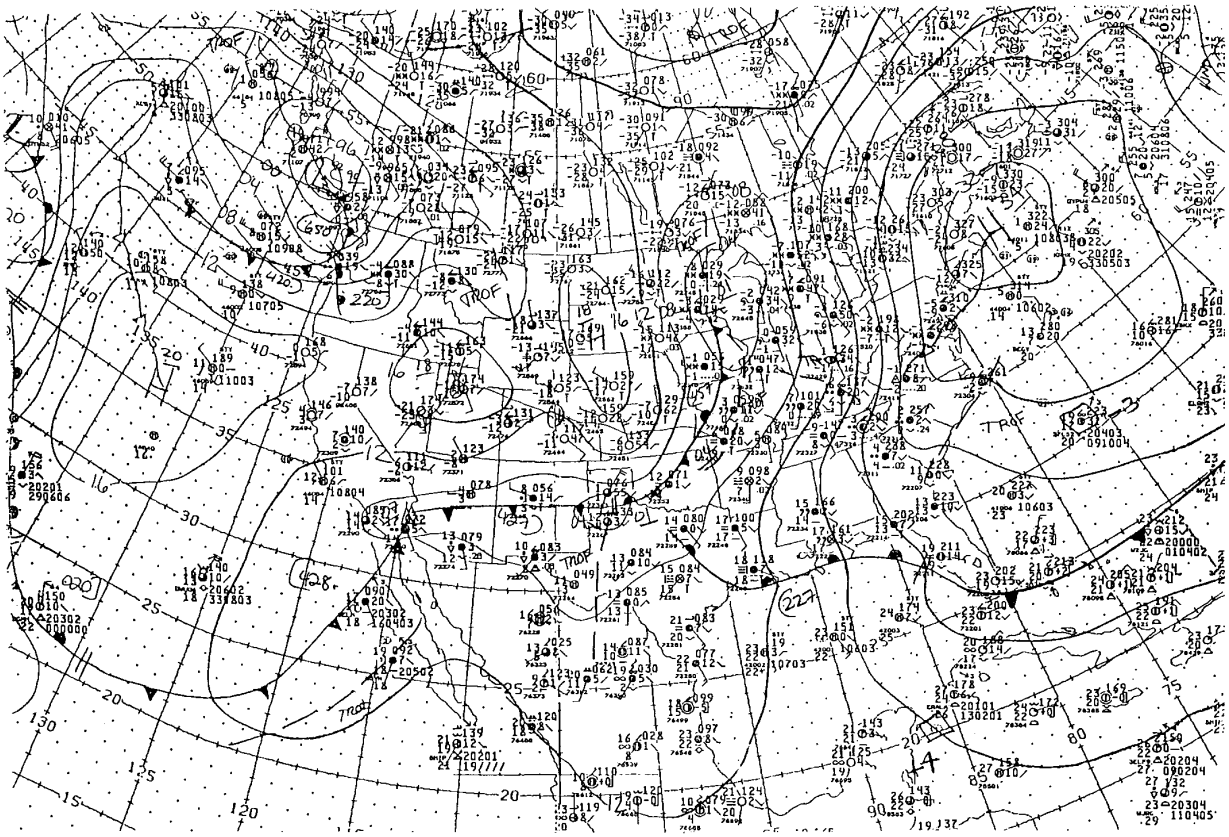

FIG. 22. As in Fig. 20 but for 1200 UTC 15 February 1995.

an analyzed central pressure of 1001 mb. Farther east, a 1034-mb anticyclone was located east of New England. A coastal front was analyzed along the Carolina coast, separating warm marine air from cooler air dammed up east of the Appalachian Mountains. The latter is reflected hydrostatically by the mean sea level pressure ridge west of the coastal front in central North and South Carolina. The 48-h eta forecasts valid at this time (Fig. 23) show that the 80-km model overdeepened the cyclone in the central United States and positioned it in Illinois. The 80-km early eta made significant errors in temperature and precipitation-type forecasts over the region. The 48-km model produced a superior forecast with a weaker cyclone centered closer to the observed position in Minnesota.

In addition to the improved forecast of the central U.S. cyclone, the 48-km model also produced a better depiction of the cold air damming situation in the mid-Atlantic states (Fig. 23). The 48-km model extended the cool air farther south than the 80-km model, as evidenced by the better positioning of the 1028-mb isobar in southern Virginia and the lower 1000–500-mb thickness in the 48-km forecast. The signature of the coastal front trough along the Carolina coast is more evident in the 48-km forecast than in the 80-km forecast.

4. Summary and future plans

A series of enhancements of the NCEP operational early eta system has been developed and tested. The most significant of these changes are the increase in horizontal grid spacing from 80 to 48 km, the introduction of a prognostic cloud scheme in the eta model physics package, and the use of a 12-h data assimilation system using the eta model to provide initial conditions. Separate impact tests of each of these components led to improvement in eta model performance, especially in the prediction of precipitation. An evaluation of the entire upgrade package in the spring of 1995 showed that the 48-km version was more skillful than the 80-km early eta in predicting both the intensity of large-scale weather systems and mesoscale precipitation events. Additionally, experiments including SSM/I IWV data in the eta ROI analysis led to minor improvement in eta model precipitation forecasts over the contiguous

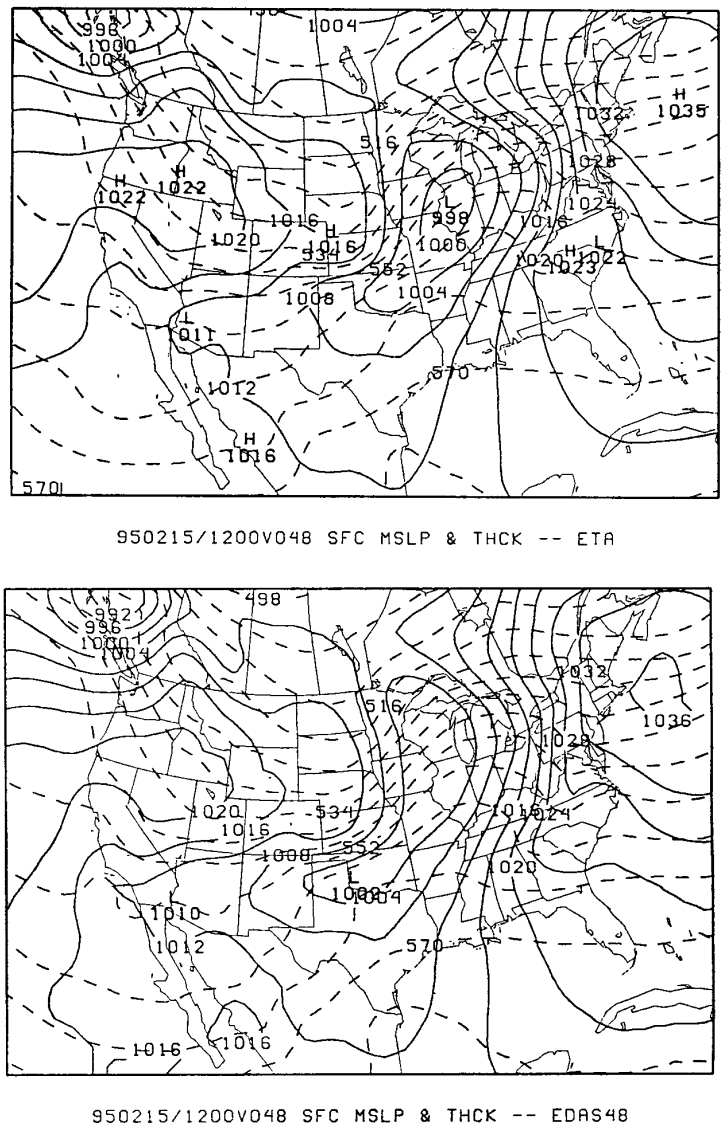

FIG. 23. As in Fig. 21 but for the 48-h forecasts valid at 1200 UTC 15 February 1995.

United States. The full upgrade package, including all the components described above, was introduced into the NCEP operational model suite at 1200 UTC 12 October 1995.

A further upgrade to the 48-km eta, not detailed in this note, was implemented at 1200 UTC 31 January 1996. This version of the model is identical to the one running in the operational mesoscale (29 km, 50 levels) eta model. In addition to the cloud scheme described in this note, this version contains a new land-surface model (Chen et al. 1996), a new viscous sublayer parameterization (Janjić 1996a), and a revised version of the Mellor–Yamada level-2.5 turbulence closure scheme (Janjić 1996b). A detailed description of the mesoscale eta system and these additional changes will be the subject of a future NCEP note.

Within the next year, NCEP plans to make two significant changes to the EDAS component of the 48-km early eta. NCEP plans to reconfigure the EDAS so that each cycle is initiated from a first guess from the previous EDAS cycle, instead of starting from the GDAS first guess. In addition, NCEP plans to replace the eta ROI analysis with a regional three-dimensional variational analysis (3DVAR). The regional 3DVAR is very similar to the system used in the GDAS (Parrish et al. 1995). Use of the 3DVAR in the EDAS will allow for assimilation of observa-

tion types (e.g., aircraft temperatures, radial winds from the WSR-88D radars) that are not easily incorporated into the ROI analysis used in the current operational EDAS.

Acknowledgments. The authors would like to thank Drs. Fedor Mesinger and Joseph Gerrity for their internal reviews of the manuscript, which greatly added to the clarity and organization of this note. The comments of Dr. John Snook and an anonymous reviewer added to the clarity of the text. We also thank Dr. Eugenia Kalnay and Dr. Ron McPherson for their continued support and encouragement of eta model development at NCEP.

APPENDIX

Definition of Objective Verification Scores for Precipitation

The equitable threat score (ETS) is defined as

$$\text{ETS} = \frac{H - CH}{F + O - H - CH},$$

where F is the number of forecast points above a threshold, O is the number of observed points above a threshold, H is the number of correctly forecasted points above a threshold, and CH is the expected number of hits in a random forecast of F points for O observed points, which is equal to

$$CH = \frac{F \times O}{\text{NUM}},$$

where NUM is the number of points in the verification domain. The ETS, through its use of CH, attempts to negate the reward achieved in a normal threat score by increasing hits via increasing the bias. It has a similar range (from 0 to 1) and interpretation as the normal threat score; that is, ETS = 1 indicates a perfect forecast.

The bias score is simply the ratio of the forecast and observed points and is defined as

$$\text{BIAS} = \frac{F}{O}.$$

If the forecast is too wet (dry), the bias score is greater (less) than one. A score of unity is a perfect forecast.

REFERENCES

Alishouse, J., S. Snyder, J. Vongsathorn, and R. Ferraro, 1990: Determinations of oceanic total precipitable water from the SSM/I. *IEEE Trans. Geosci. Remote Sens.,* **28,** 811–816.

Arakawa, A., and V. R. Lamb, 1977: Computational design of the basic dynamical processes of the UCLA general circulation model. *Methods Comput. Phys.,* **17,** 173–265.

Betts, A. K., 1986: A new convective adjustment scheme. Part I: Observational and theoretical basis. *Quart. J. Roy. Meteor. Soc.,* **112,** 677–691.

——, and M. T. Miller, 1986: A new convective adjustment scheme. Part II: Single column tests using GATE wave, BOMEX, and Arctic air-mass data. *Quart. J. Roy. Meteor. Soc.,* **112,** 693–709.

Black, T. L., 1994: The new NMC mesoscale eta model: Description and forecast examples. *Wea. Forecasting,* **9,** 265–278.

——, D. G. Deaven, and G. J. DiMego, 1993: The step-mountain eta-coordinate model: 80 km ''early'' version and objective verifications. NWS Technical Procedures Bull. 412, National Oceanic and Atmospheric Administration/National Weather Service, 31 pp. [Available from National Weather Service, Office of Meteorology, 1325 East–West Highway, Silver Spring, MD 20910.]

Chen, F., and Coauthors, 1996: Modeling of land-surface evaporation by four schemes and comparison with FIFE observations. *J. Geophys. Res.,* **101,** 7251–7268.

DiMego, G. J., 1988: The National Meteorological Center Regional Analysis System. *Mon. Wea. Rev.,* **116,** 977–1000.

——, and Coauthors, 1992: Changes to NMC's Regional Analysis and Forecast System. *Wea. Forecasting,* **7,** 185–198.

Fels, S. B., and M. D. Schwarztkopf, 1975: The simplified exchange approximation: A new method for radiative transfer calculations. *J. Atmos. Sci.,* **32,** 1475–1488.

Gandin, L., and A. H. Murphy, 1992: Equitable skill scores for categorical forecasts. *Mon. Wea. Rev.,* **120,** 361–370.

Golding, B. W., 1990: The Meteorological Office mesoscale model. *Meteor. Mag.,* **119,** 81–96.

Hamill, T. M., R. P. d'Entremont, and J. T. Bunting, 1992: A description of the air force real-time nephanalysis model. *Wea. Forecasting,* **7,** 288–306.

Hoke, J. E., N. A. Phillips, G. J. DiMego, J. J. Tuccillo, and J. G. Sela, 1989: The Regional Analysis and Forecast System of the National Meteorological Center. *Wea. Forecasting,* **4,** 323–334.

Janjić, Z. I., 1979: Forward–backward scheme modified to prevent two-grid-interval noise and its application in sigma coordinate models. *Contrib. Atmos. Phys.,* **52,** 69–84.

——, 1984: Nonlinear advection schemes and energy cascade on semi-staggered grids. *Mon. Wea. Rev.,* **112,** 1234–1245.

——, 1994: The step-mountain eta coordinate model: Further developments of the convection, viscous sublayer, and turbulence closure schemes. *Mon. Wea. Rev.,* **122,** 927–945.

——, 1996a: The surface parameterization in the NCEP eta model. *Research Activities in Atmospheric and Oceanic Modelling,* CAS/JSC Working Group on Numerical Experimentation, World Meteorological Organization, 440 pp. [Available from World Meteorological Organization, CP No. 2300, CH-1211, Geneva 2, Switzerland.]

——, 1996b: The Mellor–Yamada level 2.5 turbulence closure scheme in the NCEP eta model. *Research Activities in Atmospheric and Oceanic Modelling,* CAS/JSC Working Group on Numerical Experimentation, World Meteorological Organization, 440 pp. [Available from World Meteorological Organization, CP No. 2300, CH-1211, Geneva 2, Switzerland.]

——, F. Mesinger, and T. L. Black, 1995: The pressure advection term and additive splitting in split-explicit models. *Quart. J. Roy. Meteor. Soc.,* **121,** 953–957.

Kanamitsu, M., and Coauthors, 1991: Recent changes implemented into the global forecast system at NMC. *Wea. Forecasting,* **6,** 425–435.

Lacis, A. A., and J. E. Hansen, 1974: A parameterization of the absorption of solar radiation in the earth's atmosphere. *J. Atmos. Sci.,* **31,** 118–131.

Lin, Y., K. E. Mitchell, E. Rogers, and G. J. DiMego, 1995: Impact of satellite moisture observations on forecasts made by NMC's eta model. Preprints, *14th Conf. on Weather Analysis and Forecasting,* Dallas, TX, Amer. Meteor. Soc., 301–302.

Lobocki, L., 1993: A procedure for the derivation of surface-layer bulk relationships from simplified second-order closure models. *J. Appl. Meteor.*, **32,** 126–138.

Mellor, G. L., and T. Yamada, 1982: Development of a turbulence closure model for geophysical fluid problems. *Rev. Geophys. Space Phys.*, **20,** 851–875.

Mesinger, F., 1973: A method for construction of second-order accuracy difference schemes permitting no false two-grid interval wave in the height field. *Tellus*, **25,** 444–458.

——, 1984: A blocking technique for representation of mountains in atmospheric models. *Riv. Meteor. Aeronaut.*, **44,** 195–202.

——, 1995: The eta regional model and its performance at the U.S. National Centers for Environmental Prediction. *Int. Workshop on Limited-Area and Variable Resolution Models*, Beijing China, World Meteorological Organization, 19–28.

——, and T. L. Black, 1992: On the impact of forecast accuracy of the step-mountain (eta) vs. sigma coordinate. *Meteor. Atmos. Phys.*, **50,** 47–60.

——, and M. E. Baldwin, 1995: Skill of the eta model precipitation forecasts and its dependence on a number of model features. *Int. Symp. on the Life Cycles of Extratropical Cyclones*, Bergen, Norway, University of Bergen, 338–343.

——, S. Nič̆ković, D. Gavrilov, and D. G. Deaven, 1988: The step-mountain coordinate: Model description and performance for cases of Alpine lee cyclogenesis and a case of Appalachian redevelopment. *Mon. Wea. Rev.*, **116,** 1493–1518.

Parrish, D., J. Derber, J. Purser, W. Wu, and Z. Pu, 1995: The NMC Global Analysis System: Recent improvements and future plans. *Second Int. Symp. on Assimilation of Observations in Meteorology and Oceanography*, Tokyo, Japan, World Meteorological Organization, 403–407.

Pudykiewicz, J., R. Benoit, and J. Mailhot, 1992: Inclusion and verification of a predictive cloud-water scheme in a regional numerical weather prediction model. *Mon. Wea. Rev.*, **120,** 612–626.

Rogers, E., D. G. Deaven, and G. J. DiMego, 1995: The regional analysis system for the operational eta model: Original 80-km configuration and recent changes. *Wea. Forecasting*, **10,** 810–825.

Schaefer, J. T., 1990: The critical success index as an indicator of warning skill. *Wea. Forecasting*, **5,** 570–575.

Slingo, J. M., 1987: The development and verification of a cloud prediction scheme for the ECMWF model. *Quart. J. Roy. Meteor. Soc.*, **113,** 899–927.

Sundqvist, H., 1978: A parameterization scheme for non-convective condensation including prediction of cloud water content. *Quart. J. Roy. Meteor. Soc.*, **104,** 677–690.

——, E. Berge, and J. E. Kristjansson, 1989: Condensation and cloud studies with a mesoscale numerical prediction model. *Mon. Wea. Rev.*, **117,** 1641–1657.

van Leer, B., 1977: Towards the ultimate conservative difference scheme: A new approach to numerical convection. *J. Comput. Phys.*, **23,** 276–299.

U.S. Department of Commerce, 1994: Packing and identification of NCEP grid-point data. NCEP Office Note 84, National Oceanic and Atmospheric Administration, National Weather Service, 39 pp. [Available from National Center for Environmental Prediction, NCEP Central Operations, 5200 Auth Road, Camp Springs, MD 20746.]

Zhao, Q., T. L. Black, and M. E. Baldwin, 1996: Cloud prediction scheme in the eta model at NCEP. *Workshop on Modelling, Validation, and Assimilation of Clouds*, Reading, United Kingdom, ECMWF/GEWEX, 233–251.